Analysis of surface variables and parameterization of surface processes in HIRLAM. Part II: Seasonal assimilation experiment

B. Navascués[1], E. Rodríguez[1], J.J. Ayuso[1] and S. Järvenoja[2]
[1] Spanish Meteorological Institute (INM), P.O. Box 275, 28070 Madrid, Spain
[2] Finnish Meteorological Institute (FMI), P.O. Box 503, 00101 Helsinki, Finland

(Manuscript received 30 September 2002, in final form 22 January 2003.)

Abstract

The HIRLAM analysis of surface variables and parameterization of surface processes described in the companion paper is applied to a one year long assimilation experiment in order to evaluate the performance of the new package over an extended period covering a complete annual hydrological cycle. The time evolution of the slow evolving variables and the usage of diagnostic tools to assess the performance of the surface analysis are thoroughly discussed in the text. In particular, the usefulness of the screen level variables and soil moisture analyses to diagnose and identify model biases is highlighted. There are also sections devoted to discuss the behaviour of different tiles within a grid square and the convergence of the assimilation algorithm. The need of soil moisture analysis is justified by an additional experiment showing the appearance of long-term drift in near surface parameters when soil moisture analysis is switched off.

Contents

1 Introduction

The exchange processes between the earth surface and the atmosphere are widely recognized to be relevant at all time scales (see (Rodriguez *et al.*, 2003) and references therein). The fluxes of momentum and heat are affected both by atmospheric variables and by surface and soil characteristics. The role of soil water content has special importance, as this variable controls the partition of the net radiative energy reaching the land surface between latent and sensible heat flux turning back energy to the atmosphere. Another important feature of the soil water content is its slow time evolution. Soil water at the typical root depth (between 1 and 2 m) changes at seasonal time scales, whereas only the soil water contained in the uppermost soil layers (a few cm) responds quickly to the atmospheric forcing. For most vegetated regions the main contribution to latent heat flux comes from the transpiration of plants directly fed from soil water contained in deep layers. Therefore, the accurate evolution of this variable is crucial to properly simulate surface moisture exchange processes. The slowly evolving soil water consequently maintains a long memory which allows some degree of predictability in long run integrations.

The main aim of the yearly assimilation experiment presented here is to evaluate along a whole annual cycle the features of the surface parameterization and of the analysis of surface variables described in Part I. The technical report is organized as follows: Section 2 shortly describes the design of the experiment. In Section 3 the yearly evolution of soil variables, in particular of the slowly evolving variables, is discussed. Section 4 presents some diagnostics of the analysis of screen level variables. Special emphasis has been put on discussing the usage of diagnostic tools to identify model biases caused by deficiencies in the parameterization of physical processes. Section 5 provides diagnostics of the soil water content assimilation. The sensitivity of soil water content corrections to near surface parameters is discussed in Section 6. The effect of subgrid variability is presented in Section 7. The convergence time of the soil moisture algorithm is discussed in Section 8. Finally, results showing the drifting of soil moisture when the system evolves without soil moisture correction at each assimilation step are presented in Section 9.

2 Design of the seasonal assimilation experiment

In order to test the performance of the new surface package over an extended period covering a complete annual hydrological cycle, a one year long assimilation experiment has been run from 15 April 1995 to the end of April 1996. The starting date, when the soil reservoir has plenty of water, allows to study how the water supply to the atmosphere presents a transition from a potential rate to a different regime in which the plants are controlling the evapotranspiration according to their water availability at the root zone. The length of the experiment also allows to investigate the further evolution of the soil water, when precipitation events start to recharge the soil reservoir.

The model implementation used for this assimilation experiment is the same described in Part I for the parallel experiments using the DMR domain. The experiment has been labeled here as MOD in most graphics and maps. The HIRLAM version used now is 5.1.3 with the following features (see also Section 8 of Part I):

- Domain: Area corresponding to the DMR HIRLAM suite with a 0.5° horizontal resolution

- 166 * 130 grid points; 31 levels in the vertical
- Semi-Lagrangian advection, dt = 10 min
- Data assimilation based on optimal interpolation with 6 hours cycling
- Lateral boundary conditions: ECMWF analyses
- Period: from 15 April 1995 to 30 April 1996

3 Time evolution of soil variables

One of the main goals of the experiment was to test the time evolution of the slow variables over a complete annual cycle. Figure 1 shows the time evolution of the soil wetness index (SWI) of total soil water content averaged over three different geographical areas: Scandinavia, France and the Iberian Peninsula, respectively. SWI is defined by $(w - w_{wilt})/(w_{fc} - w_{wilt})$, where w_{fc}, w_{wilt} and w are the field capacity, the wilting point and actual soil water content, respectively. It takes the value 1 for soil water content at the field capacity, 0 for soil water content at the wilting point, negative values for soil water content below the wilting point and values bigger than one for soil water content between the field capacity and the saturation point.

In France and the Iberian Peninsula the dominant feature is the annual cycle. Higher frequency oscillations with smaller amplitude mainly corresponding to different synoptic events appear superimposed on the annual oscillation. The SWI for the Iberian Peninsula remains lower than SWI for France during the whole year. Consequently, the period in which evaporation is controlled by soil water availability is longer in the Iberian Peninsula than in France. Another observed difference between the SWI evolution in France and the Iberian Peninsula is the transition between dry and wet regimes in autumn. The steep increase of SWI in Spain around mid November is produced by a few heavy precipitation events recharging the soil water reservoir. Over France, the transition between dry and wet periods starts earlier and it is not so abrupt.

One striking feature observed in Fig. 1 is that over France the soil stays over its field capacity during several weeks in winter time. This behaviour is due to frequent episodes of rain and snow which affected France during the winter time, mainly in February. On the other hand, the soil wetness over the Scandinavian area presents a slow decrease from the climatological starting point in April 1995 until August, and then it is almost constant from autumn to early spring 1996 when soil moisture starts again to decrease. The unrealistic behaviour of SWI for the Scandinavian region has been traced back to two different sources. First, it was detected that latent heat flux over snow covered grid points was excessively large and, second, the recharge of the total soil water reservoir during the snow melting season turned out to be insufficient. The first and main source of error can be easily repaired by imposing some limitating value to the maximum roughness length allowed over snowed surfaces (see Sec. 7). In connexion with the second source of error, it must be mentioned that the current code invests most of the water from snow melting in runoff, considering that the soil below the snow package is fully impermeable because of the frozen soil moisture. It has been also checked that much more realistic values of the soil moisture annual cycle are obtained if water from snow melting is allowed to refill directly the soil water reservoirs. Probably, the best solution would be an intermediate one, *i.e.*, imposing that infiltration/runoff from snow melting would depend on the soil permeability which in turn would depend on the estimation of soil

moisture freezing. Anyway, although SWI differences can be very big, they do not affect appreciably the values of 2-metre temperature and relative humidity, as for Northern latitudes soil moisture and screen variables are very much uncoupled. After the snow melting season the soil moisture assimilation package is expected to compensate this deficit of soil water within a few days/weeks. The behaviour of the SWI in Scandinavia will be further commented in the section devoted to the differences found between the the low and high vegetation land tiles (Sec. 7).

Maps of the SWI for low vegetation and high vegetation tiles have been obtained to study the spatial distribution of the soil water content and its monthly evolution. Figure 2 shows the initial climatological distribution of the SWI in the low vegetation fraction. This mainly uniform pattern, close to field capacity, is however lost after a few assimilation cycles (see *e.g.*, Figure 3 showing SWI after five days of assimilation (*i.e.*, 20 assimilation cycles)). Two factors are mainly responsible for such modification: soil moisture assimilation and precipitation events. The heterogeneity induced by different vegetation and soil characteristics allowed for each tile also contributes, but to a lesser extent, to the rapidly changing spatial pattern of SWI.

Figure 4 depicts the daily value of 12 UTC surface temperature and mean soil temperature from ISBA scheme at 12 UTC along the assimilation experiment covering one full year (from April 1995 to April 1996). Both temperatures are averaged over all land tiles in the integration domain. The main observed feature is the annual cycle of both surface and mean soil temperatures. The figure shows the slightly delayed and attenuated response of the mean temperature to surface temperature variations. The diurnal cycle of surface temperature shows higher amplitude from spring to autumn, as it is noticeable from the larger distance between the 12 UTC surface temperature and the mean temperature curves. In winter, however, both temperatures keep very close, meaning a fairly small diurnal variation. So, surface temperature corrections are rapidly lost from spring to summer time, whereas they help to keep model values near to observations for longer forecast ranges in winter time. The big impact of temperature corrections in winter time has been checked by running one additional assimilation experiment without temperature corrections (results are not shown here). This effect is a consequence of the small forcing from the surface fluxes in the surface temperature equation (see Eq. (3) in (Rodriguez *et al.*, 2003)).

Figure 5 shows the time evolution of surface temperature at 12 and 00 UTC, together with the mean temperature for two different geographical areas, the Iberian Peninsula and Scandinavia respectively. A much higher diurnal cycle for surface temperature can be observed over the Iberian Peninsula, whereas surface temperature presents only small diurnal variations from October to the beginning of March over Scandinavia. On the other hand, the annual oscillation of the mean temperature is appreciably bigger over Scandinavia than over the Iberian peninsula. It can also be noticed that over Scandinavia some days in winter show colder surface temperatures than the mean temperature at midday. The differences between low and high vegetation land tiles temperatures mainly occuring in Southern Europe will be commented in Sec. 7.

4 Screen level analysis diagnostics

The analysis of 2-metre temperature and relative humidity averaged over land tiles has been used not only as the necessary step for the assimilation of soil variables, but also as an useful diagnostic tool to identify model biases produced by deficiencies in the parameterized physical processes. As

it was already described in the Part I, the method used for the analysis of screen level variables is Optimal Interpolation (OI) (see, *e.g.*, (Daley, 1991); (Rodriguez *et al.*, 2003)). Time series of observation departures from the background and the analysis, respectively, have been used to investigate the analysis performance and the validity of the assumptions concerning the statistics of the first guess and observation errors. As a part of it, special attention has been paid to the behaviour of the quality control checks during the analysis.

Diagnostics have been obtained separately for 00 UTC, 06 UTC, 12 UTC and 18 UTC in order to better understand the physical mechanisms and also the soil moisture assimilation features that depend strongly on the diurnal cycle of solar radiation.

Figures 6 and 7 show the evolution of the monthly averaged 2-metre temperature and relative humidity bias and standard deviation of innovations (observation minus first guess). It can be observed that there is a warm bias during daytime, maximum in mid spring 1995 that turns into cold bias (but lower) in autumn and early spring 1996. Standard deviation is of the order of $2K$ in summer and $2.5K$ from autumn to spring. The higher standard deviation occurs at 12 UTC during the whole year. Relative humidity presents small biases. At 12 UTC there is a dry bias from May to September changing to wet onwards. At 00 UTC there is a constant small wet bias. The lowest standard deviation of 2-metre relative humidity innovations corresponds to night-time, decreasing from May to June and keeping a value slighty higher than 10% in summer and autumn. During daytime the 2-metre relative humidity error increases reaching 20% in early spring, at the end of the period.

Maps of monthly mean analysis increments for 2-metre temperature reveal that the model biases in spring and autumn are mainly affecting Northern Europe (see Figs. 8 and Fig. 9 corresponding to June and October, respectively). Warm and dry systematic errors at 12 UTC, changing to cold and wet biases at night (not shown here) appear in summer over Southern Europe coastal areas. These errors may be related to a misrepresentation of local sea breeze circulations by the model due to the insufficient horizontal resolution. Wet biases are frequent in mountain regions. The model also tends to be too moist in spring and autumn over Northern Europe.

Maps of monthly rms analysis increments for 2-metre temperature show fairly homogeneous analysis increments, of the order of 1-2K in summer, as it can be observed in the Fig. 10 corresponding to August. Wider areas with increasing rms increments (2 K) take place in spring and autumn (not shown here). For 2-metre relative humidity, most of rms analysis increments remain in the range bewteen 5% and 10% (not shown here), being higher in some identified areas showing also a clear bias.

Data minus analysis differences have been obtained for both screen level parameters. Monthly bias and standard deviations of these residuals for 2-metre temperature and relative humidity are shown in Figures 11 and 12, respectively. In order to account for the correction of temperature due to the difference between the model and the station height a constant standard lapse rate of $0.0065K/m$ has been applied. It can be seen that standard deviations for these residuals are of the order of $1K$ and 6%, respectively, at all times of the day and for all seasons. Biases are insignificant.

As stated by Talagrand (1999), an objective assesment of the quality of an estimation procedure can be made only against observations which are independent of the information used in the estimation process. Data minus analysis differences are nevertheless a powerful diagnostic tool to evaluate the assimilation system performance based on a linear objective analysis algorithm,

as discussed by some authors (see *e.g.*, (Hollingsworth and Lonnberg, 1989), (Talagrand, 1999) and (Talagrand and Bouttier, 2000)). They also proposed diagnostics for different linear analysis algorithms that were already tried in the past for a statistical interpolation analysis method by Hollingsworth and Lonnberg (1989) and more recently for a variational assimilation system by, *e.g.*, Bouttier (2001). The good coverage of data at screen level over Europe allows the evaluation of the internal consistency of the data assimilation algorithm. Hollingsworth and Lonnberg (1989) already mentioned that bulk statistics on the mean and standard deviation of the residuals had proved to be very useful in diagnosing "zero order" problems with data of assimilation systems. They have called "efficient" an analysis system that fits data to within observational accuracy. In this respect, Talagrand (1999) also shows that as the estimation error decreases (for instance due to an increasing amount of observations) the magnitude of the residuals increases asimptotically to the level of observation error. On the other hand, if background and observation errors are not mutually correlated, the variance of innovations is the sum of both observations and first guess error variances (Daley, 1991). Therefore, a large sample of both innovations and residuals provides useful information for preliminary testing the validity of the assumptions of the error statistics in the analysis. As it was mentioned by Rodriguez *et al.* (2003), both observation and background errors and the structure function characteristic length scales were tuned a priori, because no time series of background departures with the new surface parameterization were available. Values were assigned on the basis of the error statistics from the old surface scheme, and they were further modified in order to produce realistic quality control decisions. In particular, observation error standard deviations used for 2-metre temperature and relative humidity are $1K$ and 10%, respectively. So, according to the figures of residuals and innovations, the value for the relative humidity observation error might be overestimated. The specified values for background errors are $1.5K$ and 15%. Looking at Figures 6 and 7 showing the evolution of monthly averages of bias and standard deviation of innovations, it seems reasonable to introduce a seasonal dependence on the assumed background errors, at least for the case of 2-metre relative humidity. On the other hand, it may be needed to substract the daytime bias at least over some geographical areas showing significant systematic errors, provided we are assuming unbiased background departures in the OI analysis.

Most of modern assimilation algorithms rely on the normal distribution of background and observation random errors. As it is shown by Lorenc (1986) using Bayesian arguments, the *a posteriori* analysis probability distribution function produced by the minimum variance best estimate searched by the OI algorithm is also Gaussian. An additional diagnostic to assess the performance of the analysis algorithm consists of obtaining histograms of both background and analysis departures. Such histograms have been produced by using all observations accepted by the analysis every month at each of the analysis times: 00, 06, 12 and 18 UTC. The histograms in Figures 13 and 14 show background and analysis departures, respectively, for 2-metre temperature in November 1995 at 00 UTC. Both distributions show symmetric and nearly Gaussian appearance, as expected specially for that month at 00 UTC due to the good agreement between the theoretical statistics applied and the *a posteriori* data minus analysis differences. Analysis departures histograms for both 2-metre temperature and relative humidity at different months and times of the day show to be close to Gaussian as the corresponding background departures do not present asymmetric tails. In general, the model bias is reasonably small. The data minus analysis distribution results turn out to be not far from Gaussian.

One key point of any analysis system is the quality control of observations. Quality control decisions are particularly affected by any weakness in the specification of the observation and first guess errors statistics, and it has been a cause of concern during the development and preliminary tests of the whole system. Length scales had to be reduced and observations to guess errors ratio

smoothed with respect to the values derived from the old surface scheme error statistics to get a reasonable small number of rejections. During this one full year assimilation experiment it has been found that the amount of observations rejected during any of first guess or OI checks is around 1% of the total data.

Histograms of the background departures for 2-metre temperature gross errors present near flat distributions, as can be observed in the example of Fig. 15 corresponding to the rejected observations in September 1995 at 18 UTC. The relative frequency has been calculated over the total number of rejections. Data in bins with the highest absolute departures correspond to observations rejected by the first guess check, whereas observations in the central bins were rejected during the OI check. The corresponding analysis departure histogram is shown in Fig. 16. As expected, in general the *a posteriori* analysis increases the distance to the gross errors dataset. Some rejected data are only 2.5 K apart from the analysis. This seems to indicate a very small estimation error over certain areas.

5 Soil moisture assimilation diagnostics

Maps of monthly mean and rms corrections of soil water content have been produced for both the low and high vegetation tiles to assess the behaviour of the soil moisture assimilation system. The occurrence of the different constraints preventing soil moisture assimilation has been additionally studied.

The total soil water corrections averaged on monthly basis can also help to detect biases coming from the physics. Maps in Fig. 17 show monthly averaged total soil water corrections for the low vegetation tile over the Iberian Peninsula corresponding to the months of August and October 1995. Figure 18 is the mean soil water correction corresponding to August 1995 for the European area. The magnitude of the monthly mean corrections keeps within the range [-5,6] mm. Visual inspection does not allow to detect a clear predominance of positive or negative areas. Perhaps it can only be said for this specific month of August 1995 that the model shows some slight tendency towards excessively wet soil over Ireland, British Isles and Northwest of France, which is compensated by negative soil water corrections. The rest of the area was overall positively corrected for soil water, meaning a model trend towards too dry soils.

Maps of monthly rms difference of total soil water corrections show, as expected, a seasonal variation, with the highest corrections occuring in summer time. Figure 19 shows the monthly rms difference of total soil water corrections for October and August 1995 over the the Iberian Peninsula area. In general, corrections do not exceed 9 mm in summer. The spatial distribution is not homogeneous, as soil water assimilation increments depend strongly on the vegetation and soil characteristics, in particular on vegetation coverage, which presents maximum values from July to September in many vegetation types. Consequently, corrections can reach up to 10-12 mm over some crop areas along the summer time. In spring and autumn soil water assimilation increments remain below 3 mm.

Changes produced by the soil moisture assimilation scheme are potentially maximum in summer. However, as it has been already documented, a number of restrictions are imposed to produce soil moisture corrections only in situations where the 2-metre temperature and relative humidity are

sensitive to soil water content. Figure 20 shows the number of 12 UTC cycles including soil water corrections for each grid point and for the months of June and October 1995 over the Iberian peninsula. The check on the opposite sign of 2-metre temperature and relative humidity innovations puts the upper bound to the possible number of effective soil moisture assimilation cycles. Nevertheless, the additional check allowing corrections only when soil water content is within the range between 0.1 times the wilting point and the field capacity seems to be more efficient in reducing the number of soil moisture assimilation cycles. It is important to mention that the soil moisture correction algorithm allows, however, to add water even if the soil reservoir is below the wilting point. This exception was introduced in order to dispose of a quick mechanism to refill the water reservoir in cases of regions with very sporadic precipitation events. When soil moisture is wetter than field capacity, the physics has already two efficient mechanisms to decrease soil moisture, namely, drainage and evapotranspiration. In particular, drainage relaxes soil water to the field capacity after a few days in absence of precipitation. Therefore, the soil moisture analysis does not need to act in the range between field capacity and saturation either to add or to remove water. Maps of soil wetness index over Spain show that the soil water content is always above its field capacity in the Pyrenees and Cantabric mountains located in Northern Spain, whereas in many areas in Southern Spain soil water is still far below the wilting point in autumn. The constraints linked to the synoptic conditions (no precipitation, low wind speed, no snow) are not only responsible for switching-off soil moisture corrections but also for reducing significantly the magnitude of the assimilation increments. The low cloudiness condition decreases only very slightly the soil moisture corrections. In particular, it has been observed that the persistent precipitation over the mountains is preventing the activation of soil moisture assimilation in some specific areas of the Iberian Peninsula. These synoptic restrictions also contribute to produce a seasonal and latitudinal variation in the number of active soil moisture assimilation cycles, with fewer corrections in the most Nordic regions, as it is observed in Fig. 21.

6 Sensitivity of soil moisture corrections to near surface parameters

The linear relationship between 2-metre temperature and relative humidity errors and soil water corrections has additionally been explored. Monthly mean biases and rms differences of analysis increments in screen level parameters might give some indication of sign, size and distribution of soil moisture assimilation increments. In particular, it is worthwhile to see how model biases influence the soil moisture assimilation. One would expect that, in principle, the soil moisture analysis increments will reproduce near surface parameter error patterns. However, in practice, it is not straightforward to trace back soil water corrections to errors of atmospheric variables. The main reason is that local solar time and vegetation properties are modulating soil moisture corrections. The vegetation characteristics present monthly variations and, as it has been already mentioned a wide spatial variability of land use classes is allowed. Furthermore, there are a number of different restrictions that may lead to null assimilation increments.

Fig. 22 shows the rms analysis increments of 2-metre temperature and relative humidity and total soil water content in the low vegetation tile for July 1995 at 12 UTC over Spain and Portugal. It illustrates the reaction of soil moisture assimilation to errors in near surface parameters. The gaps appearing over mountain regions in the soil water corrections map mean that during the whole month corrections were never applied to those grid points. The reason for this is that soil water

content was always above field capacity there. It may be also observed that the highest soil water analysis increments do not correspond to high errors of near surface parameters. In particular, soil moisture corrections of 7-9 mm appear in a wide area in the Northern inland part of the Iberian Peninsula and these values are associated with small 2-metre temperature and relative humidity errors. The vegetation type assigned to each grid point for the low vegetation tile appears also plotted in Fig. 22 (lower right). Table 1 shows land use class, vegetation coverage, leaf area index and minimum stomatal resistance corresponding to the month of July for the existing low vegetation types over Spain and Portugal. It can be seen that the highest soil moisture increments occur over crop areas. Furthermore, looking at Table 1, and as expected according to the formulation of the soil moisture optimal coefficients (see Rodriguez *et al.* (2003)), it may be observed that vegetation coverage is the main parameter determining the size of soil moisture corrections. This vegetation characteristic together with the leaf area index to minimum stomatal resistance ratio explain fairly well the screen level errors maps.

Table 1: Values of low vegetation parameters (July).

Index	Vegetation type	Veg. cover	Rsmin(s/m)	LAI(m^2/m^2)
1	crops	0.80	40.	2.0
2	short grass	0.85	40.	1.0
7	tall grass	0.30	40.	1.0
10	irrigated crop	0.85	150.	1.0
11	semi desert	0.10	150.	0.5
16	evergreen shrub	0.50	150.	3.0
17	decidious shrub	0.50	150.	3.0

In spite of the difficulties pointed out, and for large spatial scales, it has been also observed that soil moisture assimilation is used to compensate biases detected during the surface analysis step. This effect, however, is very much smoothed by the seasonal variation of soil moisture assimilation coefficients. It can be mentioned that the systematic drying caused by the soil water assimilation algorithm (observed in the map of mean soil water corrections for October 1995, not shown here) is the response to the cold bias seen in Fig. 8 over Northern and Eastern Europe. Another typical feature ocurring over some coastal areas in summer time is that high rms of soil water corrections are associated with dry and warm biases at midday, changing to wet and cold during night-time. In these cases soil water corrections are trying to compensate the lack of representation of sea breezes in the model. The rms analysis increments maps in Fig. 22 show this behaviour over the Iberian Peninsula. Along the west coast, in the Strait of Gibraltar and in some Mediterranean coastal areas high 2-metre temperature and relative humidity errors are producing relatively high corrections of soil moisture. Their magnitude is, however, limited by the characteristics of the vegetation type beneath.

Another aspect studied is the relative impact of the 2-metre temperature and relative humidity errors. In general, it has been observed that both variables contribute with similar weight to produce the analysis increment of soil water content. It should be also taken into account that, in order to remove from the 2-metre temperature error biases coming from other model deficiencies, the analysis increment is filtered efficiently before being used to correct the soil water content (see (Rodriguez *et al.*, 2003)).

7 Heterogeneity

Some preliminary diagnostics have been produced to analyze the performance of the mosaic approach used by the new surface parameterization. In particular, it is interesting to assess differences in soil moisture and temperature for low and high vegetation land tiles within the same grid square. Some results will be presented here to illustrate the effect of subgrid variability referred to two different geographical areas representing the South and the North of Europe: the Iberian Peninsula and Scandinavia.

Time evolution of SWI and soil temperatures averaged for both low vegetation and forest fractions corresponding to all points within the Iberian Peninsula area are represented in Figures 23 and 24, respectively. Surface temperature at 12 UTC has been plotted in addition to mean temperature. It may be observed that soil water content decreases faster in the low vegetation tile, keeping forest areas wetter than low vegetation areas from spring to early winter. On the other hand, and consistently with the previous fact, mean temperature over low vegetation tiles is sligthly warmer (of the order of 1 K) than over the forest fraction from spring to autumn. From Fig. 24 it can be seen that the magnitude of the diurnal cycle of the surface temperature is minimum in winter with only small differences between both land fractions. Surface temperature is colder over the forest fraction the rest of the year, especially in spring 1996 when SWI for both land tiles do not differ so much as happens in summer 1995. This could be related with the fact that the vegetation cover is small over the low vegetation tile at this time of the year. Consequently, less evapotranspiration is produced (as compared with the forest fraction) and therefore a different partition of the surface net radiation into latent and sensible heat takes place. However, as values assigned to vegetation coverage are high for both land fractions (low vegetation and forest) during summer months, the less soil moisture available at the root zone for the low vegetation tile is the predominant cause of the reduced evapotranspiration. The effect of the usually smaller stomatal resistance to canopy transpiration over the low vegetation tile tries to compensate such less favoured evapotranspiration.

The same type of figures have been also obtained for Scandinavia (Figs. 25 and 26). Looking at the evolution of soil moisture, the first striking feature is the clearly different behaviour of soil water content over both fractions. In the low vegetation tile, SWI decreases slightly in July and August, then recovers rapidly to the field capacity in October, and keeps almost constant value until next spring. However, the forest fraction shows a slow but continuous drying along the whole period. Several factors could contribute to it. As we have already commented in previous sections, the screen level parameter analysis shows a cold daytime bias in the model from October onwards mainly in Sweden and Finland where forest fraction is dominant. In the case of evergreen trees, vegetation coverage is very high along the whole year. This means that over snowfree areas the soil moisture assimilation algorithm will try to compensate this bias by removing water from the soil, whenever synoptic conditions are favourable. On the other hand, excessively high latent heat flux has been observed over snow-covered areas, possibly due to the too high roughness length assigned to forest areas with snow (as it was already commented in Sec.3). Very recent tests proposed by Gollvik (personal communication) in the sense of reducing the roughness length for snow-covered areas have very much decreased latent heat flux in March, removing the cold bias observed before. The ERA 40 surface scheme developed at ECMWF introduces an special treatment in the calculation of evaporation over high vegetation with snow underneath (van den Hurk *et al.*, 2000). Evaporation from snow lying under the vegetation uses an additional constant aerodynamic resistance. This approach could be an alternative to modify the roughness length over snow-covered areas.

Figure 26 figure shows the time evolution of soil temperatures for Scandinavia. There is no significant difference between low and high vegetation tiles in this case. This indicates the low sensitivity to soil water content variations. The amplitude of the diurnal cycle in surface temperature, as expected, is much smaller than in Southern Europe.

As it has been already thoroughly described in Part I (see (Rodriguez *et al.*, 2003)) different tiles within a grid square evolve independently driven by the atmospheric forcing. Also different soil moisture corrections are applied depending on the different vegetation and soil properties of each tile. Consequently, the value of soil moisture may appreciably diverge between different tiles inside a grid box (as it has been already illustrated by Figures 23 and 25). One interesting problem in connexion with such subgrid variability of soil moisture would be the estimation of its variance. Most of the grid points located over Europe have contributions from the low vegetation and forest tiles. In order to have a very first idea of the subgrid variability of soil moisture, difference of soil moisture between low and high vegetation tiles has been plotted (see Figs. 27-30) for four days corresponding to different seasons over an area covering the Iberian peninsula. Soil depths corresponding to all land fractions have been previously normalized to 1 m. The behaviour of the subgrid soil moisture variability over other European regions does not differ very much from this selected area. The pattern of soil moisture differences is very irregular for all selected days. The differences increase from May (Fig. 27) to October (Fig. 29). Episodes of heavy precipitation recharge equally both tiles and consequently tend to smooth soil moisture differences, as both tiles usually reach saturation at the same time. This is the case of 2nd February (Fig. 30) where the lack of differences in the western part of the Iberian peninsula matches very well with the map of accumulated precipitation (not shown here) over the previous few weeks. Differences of up to 20 mm between both tiles are not uncommon. It should be stressed that although the differences in soil moisture between the low and high vegetation tiles may sometimes be quite big, the corresponding effect on 2-metre temperature is rather moderate for most of the cases. The corresponding maps of differences for 2-metre temperature hardly reach values bigger that 1 K (not shown here).

8 Soil moisture convergence

One crucial point of the soil moisture assimilation algorithm is the convergence time *i.e.*, the period or number of assimilation cycles needed to reach realistic soil water content when starting from some climatological values which may be excessively wet or dry. Mahfouf (1991) and Bouttier *et al.* (1993a, 1993b) have shown that after two days of assimilation cycling their algorithm was able to converge to the correct soil water content.

In an operational context it may be very useful to have an estimation of the time period needed to get such convergence when the model run is "cold-started" from the climatological soil water content. For this purpose, a new experiment (named DMN) has been run starting from the 1st July 1995 and was initialized with the climatological soil water content. Values of SWI from this experiment have been compared with the corresponding ones from the seasonal experiment started in April 1995. Both experiments have the same soil moisture assimilation and they only differ in the starting date of the assimilation cycle. Figure 31 shows the time evolution of SWI in July 1995 for three different regions (Scandinavia, France and Iberian Peninsula). It may be observed that convergence is attained after one week over Scandinavia, after 3-4 weeks over France and even after a longer period the Iberian Peninsula. In order to understand the somehow different convergence

in Southern Europe, it should be remembered that the soil moisture assimilation algorithm is only active when soil moisture is within the range between field capacity and wilting point. Some areas in Spain have already reached the wilting point in July and the assimilation algorithm is no more removing soil water there. On the other hand, the unrealistic precipitation over the mountain regions has caused the filling of the soil water reservoir for the integration starting in April 1995, surpassing over some points the field capacity and consequently switching-off also the assimilation algorithm. It has also been observed that some grid points over the Iberian peninsula show a very slow evolution of soil wetness during dry periods, and therefore they keep a long memory of the initial conditions. This fact seems to be related to the underlying physiography. Some land use classes (*e.g.*, semi-desert, tall grass) only allow an insignificant or very small soil moisture correction in the assimilation step and negligible evapotranspiration during the model integration. This is due to the low value of the assigned vegetation coverage corresponding to the month of July (see Table 1). The fraction of forest, in general, presents a slower convergence of soil water content due to its higher minimum stomatal resistance and the consequent reduction of the soil moisture optimal coefficients. The soil moisture analysis increments are, as expected, much higher for the first days of July for the experiment started on 1 July.

A general feature for the three areas here considered is that the initial climatological soil moisture seems to be excessively dry in July. If the experiment would have started from a wetter first guess in July, both the model and the assimilation algorithm would have acted in the same direction decreasing soil water content and favouring a faster convergence. Also, the ocurrence of frequent and generalized rain events would probably help to attain a quicker convergence. In spite of the experiment has started from a not very realistic soil water content, the results presented demonstrate the robustness of the procedure to get correct soil moisture within a few days. Nevertheless, longer time periods might be needed in Southern Europe if the model is initialised from climatology in summertime.

9 Experiment without soil moisture assimilation: drifting

The main role of soil water content corrections is to prevent undesired long-term drifting of soil water caused by inaccuracies of the physics package. Biases of predicted precipitation, evapotranspiration or radiation can produce unrealistic values of soil water content after a certain number of assimilation cycles. As the effect of such biases is accumulative, drifting of soil water could reach unrealistic values on a seasonal time scale.

The ECMWF model suffered a serious bias in surface parameters in spring 1994 due to soil water drifting. The problem seemed to be related with an excessive shortwave radiation reaching the surface due to a negative bias in cloud cover (Viterbo, 1996). The quick fix then applied was to initialise soil moisture to field capacity over vegetated areas. As a consequence of this drift, a simple nudging method of soil water assimilation was developed and implemented at the end of 1994. In that method, lowest level humidity analysis increments were used to correct soil water content in the root layer.

In order to complement the diagnostics obtained from the seasonal assimilation experiment and to improve our knowledge of the whole system described in the Part I of this paper, an additional experiment (named DMW) without soil moisture assimilation was started on the 1st of July 1995.

This experiment is compared with the experiment DMN (described in Section 8) starting from the same date but with the soil moisture assimilation switched on. Figure 32 shows the time evolution of 2-metre relative humidity H+6 forecast bias and rms error. Verification scores were calculated by using all available observations in the model area. The divergence of both experiments are clearly noticeable after one week of assimilation. The 2-metre relative humidity is directly related to surface evapotranspiration and thus to soil water content at the root zone. Model drift increasing with time towards dry bias is evident. There is also an associated warm bias degrading scores for 2-metre temperature (not shown here).

This result confirms that soil moisture assimilation is essential to keep a reasonable time evolution of total soil water content, and to avoid a possible drift in model surface parameters. It also might reflect some deficient forcing from other physical processes into surface parameterization.

10 Summary

The new package for the analysis of surface variables and parameterization of surface processes has been evaluated in a year long assimilation experiment:

- The evolution of soil moisture coming both from the physics and the assimilation contributions for different European reagions has been assessed and thoroughly discussed in the text. Also the evolution of mean temperature and the amplitude of the diurnal cycle has been discussed for different regions.
- Extensive diagnostics of analysis of the screen level variables has been presented to validate independently the performance of the 2-metre temperature and relative humidity analysis.
- Maps of monthly mean and rms corrections of soil water content have been also produced to estimate the behaviour of the soil moisture assimilation system for different regions and seasons.
- The sensitivity of soil moisture corrections against 2-metre temperature and relative humidity errors has been discussed in depth. The role of vegetation characteristics has been specially emphasized.
- The crucial issue of the convergence of soil moisture when starting from unrealistic soil moisture values has been discussed. The convergence of soil moisture shows some latitudinal dependence.
- The heterogeneity aspects have been considered by studying separately the behaviour of different tiles within a grid square. It has been shown that the diverging evolution of different tiles within a grid square can have a visible effect on the seasonal time scale.

Finally, one additional experiment has been conducted showing that soil moisture drifts after a few weeks of integration when the soil moisture correction is switched off in the analysis step. This last result demonstrates that the soil moisture analysis is an essential component of the system described in Part I.

Acknowledgments. The authors are very grateful to Björn Bringfelt, who first started a preliminary version of the HIRLAM tiled surface scheme and proposed many of the ideas still present in the current code, to Bart van den Hurk, who re-coded a substantial part of parameterization part, to Dominique Giard, Eric Bazile and Gianpaolo Balsamo, for the very useful exchange of ideas and the stimulating years of joint work, to Stefan Gollvik, who has shed light on the problems related with the snow formulation, to Anne Jochum, who has scrutinized the manuscript and suggested improvements to the text and to many other HIRLAM colleagues (too many to be named here) for the illuminating discussions which have helped us to improve the formulation of the code. Finally, we also thank to Per Unden and one anonymous reviewer for their constructive comments on the original manuscript.

References

1. Bouttier F. 2001. The use of profiler data at ECMWF. *Technical Memorandum No.***331**, ECMWF Research Department. (Available from ECMWF, Shinfield Park, Reading, Berkshire RG2 9AX, UK.).

2. Bouttier F., Mahfouf, J.-F. and Noilhan, J. 1993a. Sequential Assimilation of Soil Moisture from Atmospheric Low-Level Parameters. Part I: Sensitivity and Calibration Studies. *J. Appl. Meteor.*, **32**, 1335-1351.

3. Bouttier F., Mahfouf, J.-F. and Noilhan, J. 1993b. Sequential Assimilation of Soil Moisture from Atmospheric Low-Level Parameters. Part II: Implementation in a Mesoscale Model. *J. Appl. Meteor.*, **32**, 1352-1364.

4. Daley, R. 1991. *Atmospheric data analysis.* Cambridge Atmospheric and Space Science Series, Cambridge Univ. Press. ISBN 0.521-38215-7, 457 pp.

5. Hollingsworth, A. and Lonnberg, P. 1989. The verification of Objective Analyses: Diagnostics of Analysis System Performance. *Meteorol. Atmos. Phys.*, **40**, 3-27.

6. van den Hurk, B.J.J.M, Viterbo, P., Beljaars, A.C.M. and Betts, A.K. 2000. Offline validation of the ERA40 surface scheme. *Technical Memorandum No.***295**, ECMWF. (Available from ECMWF, Shinfield Park, Reading, Berkshire RG2 9AX, UK.).

7. Lorenc, A.C. 1986. Analysis methods for numerical weather prediction. *Quart. J. Roy. Meteor. Soc.*, **112**, 1177-1194.

8. Mahfouf, J.-F. 1991. Analysis of soil moisture from near-surface parameters: a feasibility study. *J. Appl. Meteorol.*,**30**, 1534-1547.

9. Rodriguez, E., Navascues, B., Ayuso, J.J. and Järvenoja, S. 2003. Analysis of surface variables and parameterization of surface processes in HIRLAM. Part I: Approach and verification by parallel runs. *HIRLAM Technical Report No 58*, Norrköping, Sweden. [Available from P. Unden, SMHI, S-60176 Norrköping, Sweden].

10. Talagrand, O., 1999. A posteriori evaluation and verification of analysis and assimilation algorithms. *Proceedings of the ECMWF Workshop on Diagnosis of Data Assimilation Systems. ECMWF, Reading, November 1998, 17-28.* (Available from ECMWF, Shinfield Park, Reading, Berkshire RG2 9AX, UK.).

11. Talagrand, O. and Bouttier, F. 2000. Internal diagnostics of data assimilation systems. *Proceedings of the ECMWF Seminar on Diagnosis of Models and Data Assimilation. ECMWF, Reading, September 1999, 407-409.* (Available from ECMWF, Shinfield Park, Reading, Berkshire RG2 9AX, UK.).

12. Viterbo, P. 1996. The representation of surface processes in general circulation models. Thesis submitted for the degree of Doutor em Fisica of the University of Lisbon. ECMWF. (Available from ECMWF, Shinfield Park, Reading, Berkshire RG2 9AX, UK.).

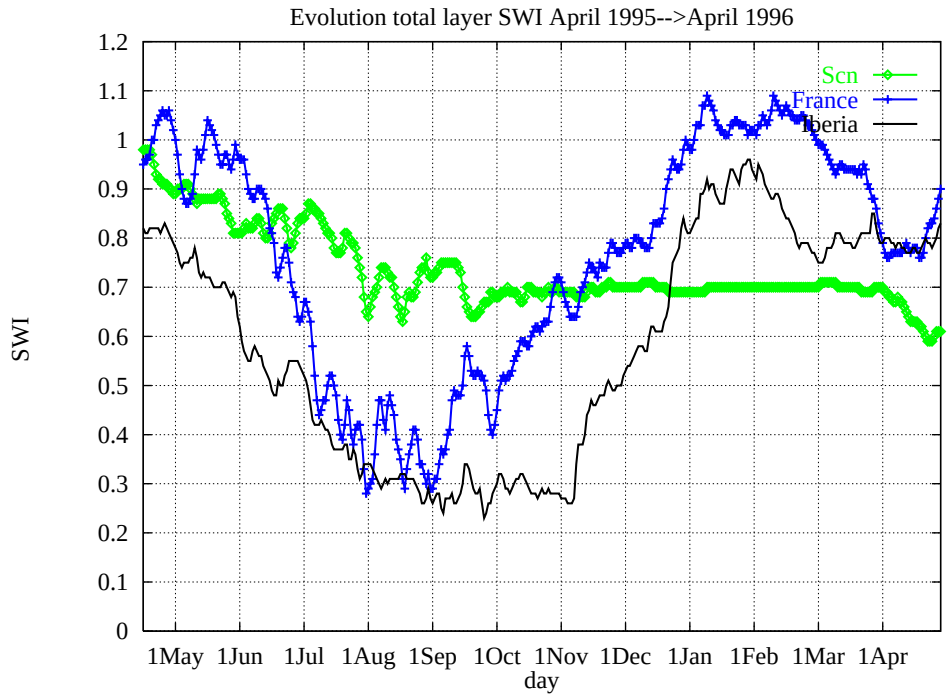

Figure 1: Daily evolution of soil wetness index averaged for all grid points in some European areas: Spain (35.N, 44.N, 4.E, -10.E), France (44.N, 50.N, 8.E, -2.E) and Scandinavia (55.N, 70.N, 32.E, 8.E). Only daily 12 UTC analysis values are used. The assimilation experiment covers one full year (from 15 April 1995 to 30 April 1996).

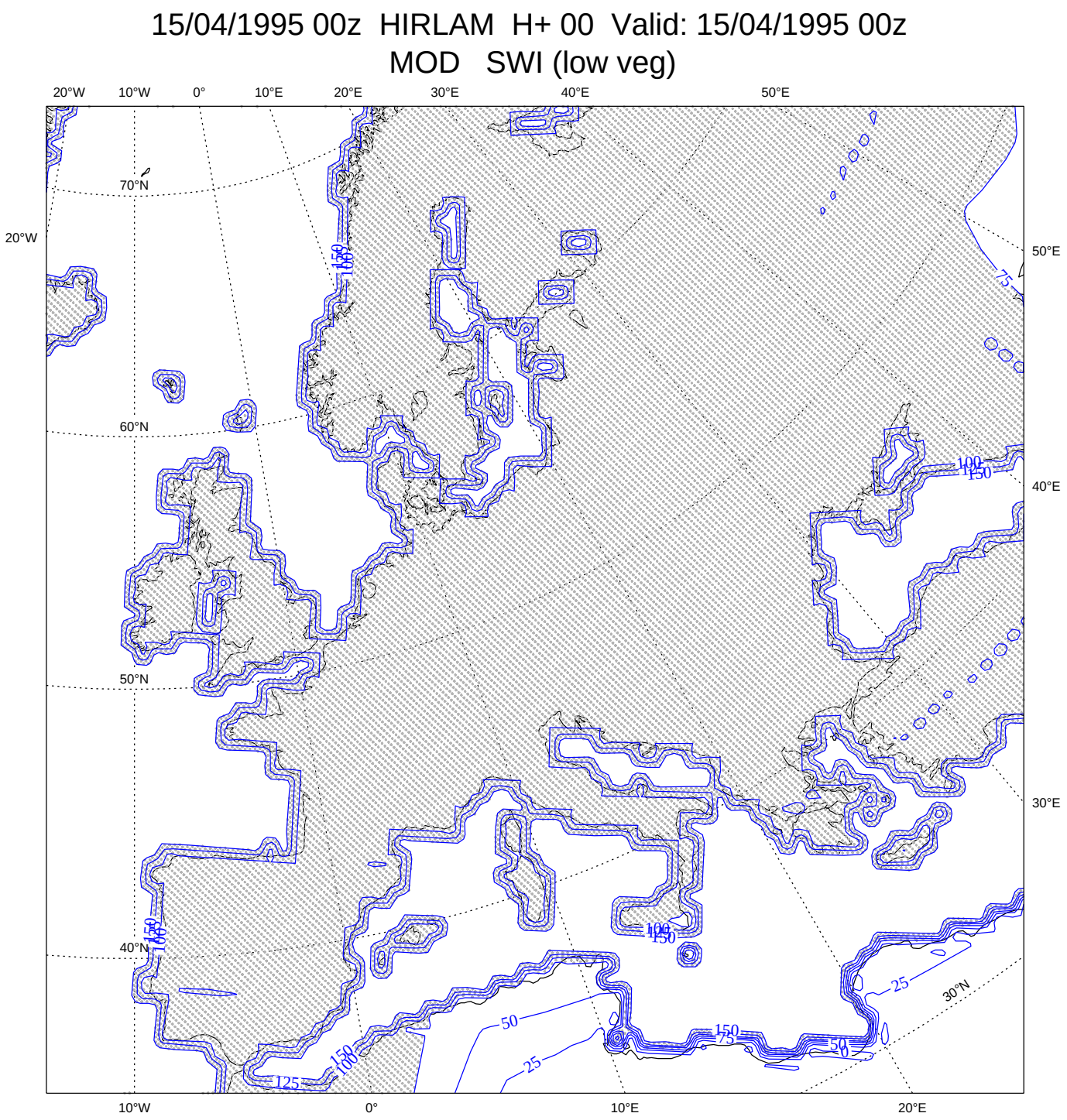

Figure 2: Climatological soil wetness index (multiplied by 100) in April over the low vegetation fraction. Contouring interval: 25. Shading in the range 75-150. Field capacity and wilting point correspond to the 100 and 0 contour lines, respectively.

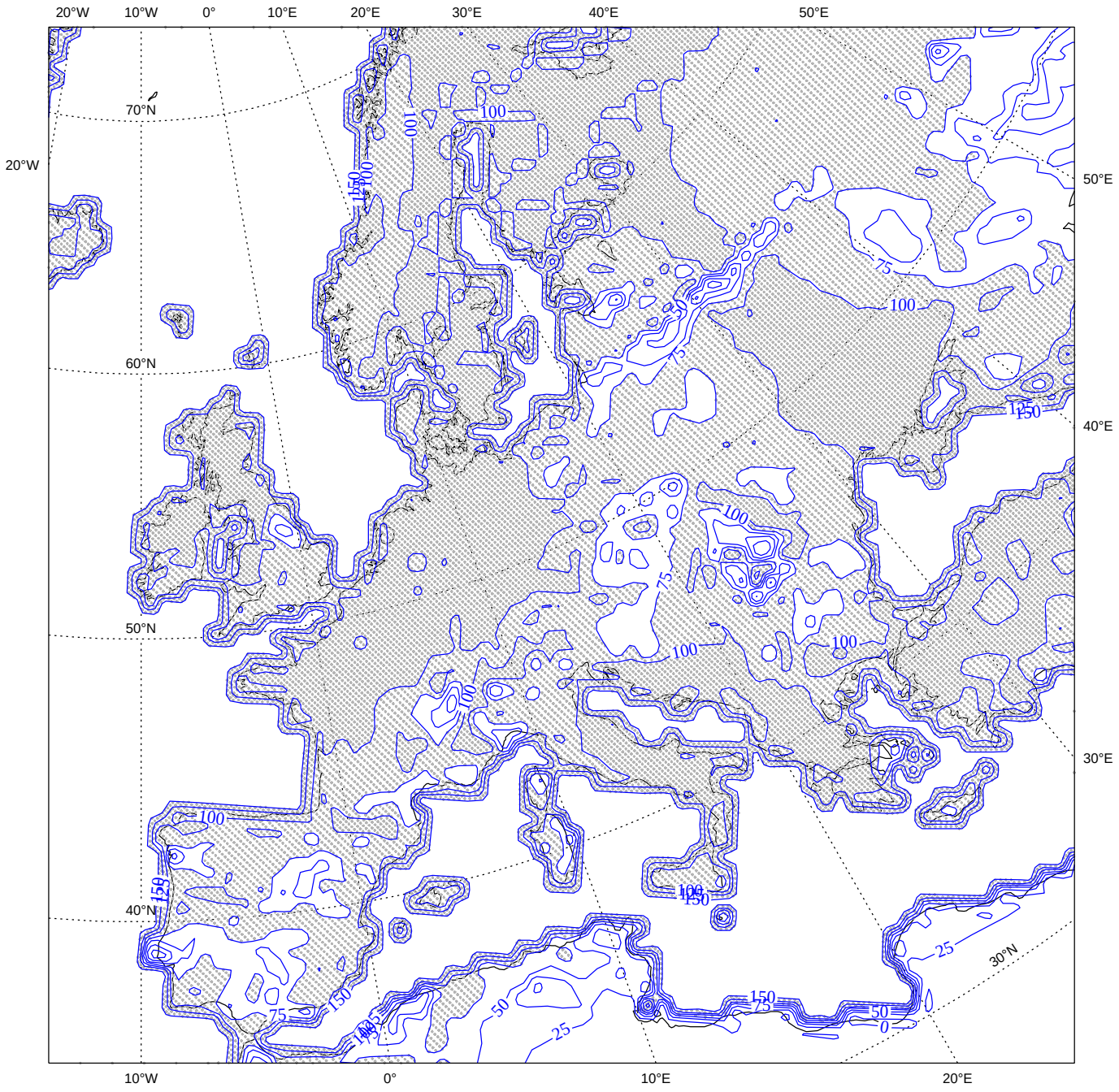

Figure 3: As in Fig. 2, but for 20th April 1995 (after 20 assimilation cycles).

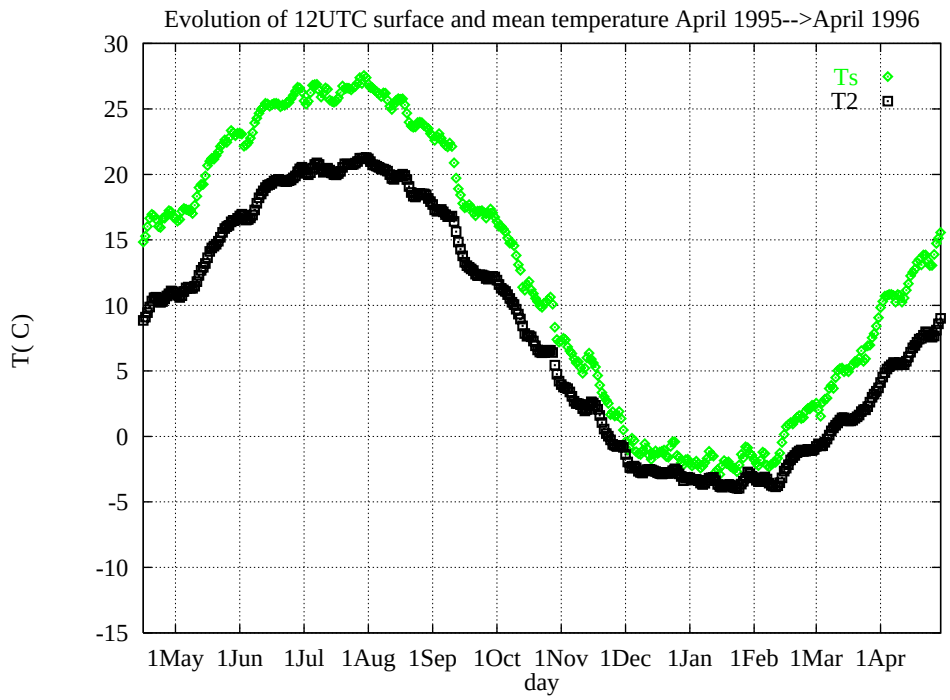

Figure 4: Daily evolution of 12 UTC surface (T_s) and mean (T_2) soil temperatures averaged for all land grid points in the model area as seen by 12 UTC analysis. The assimilation experiment covers one full year (from 15 April 1995 to 30 April 1996).

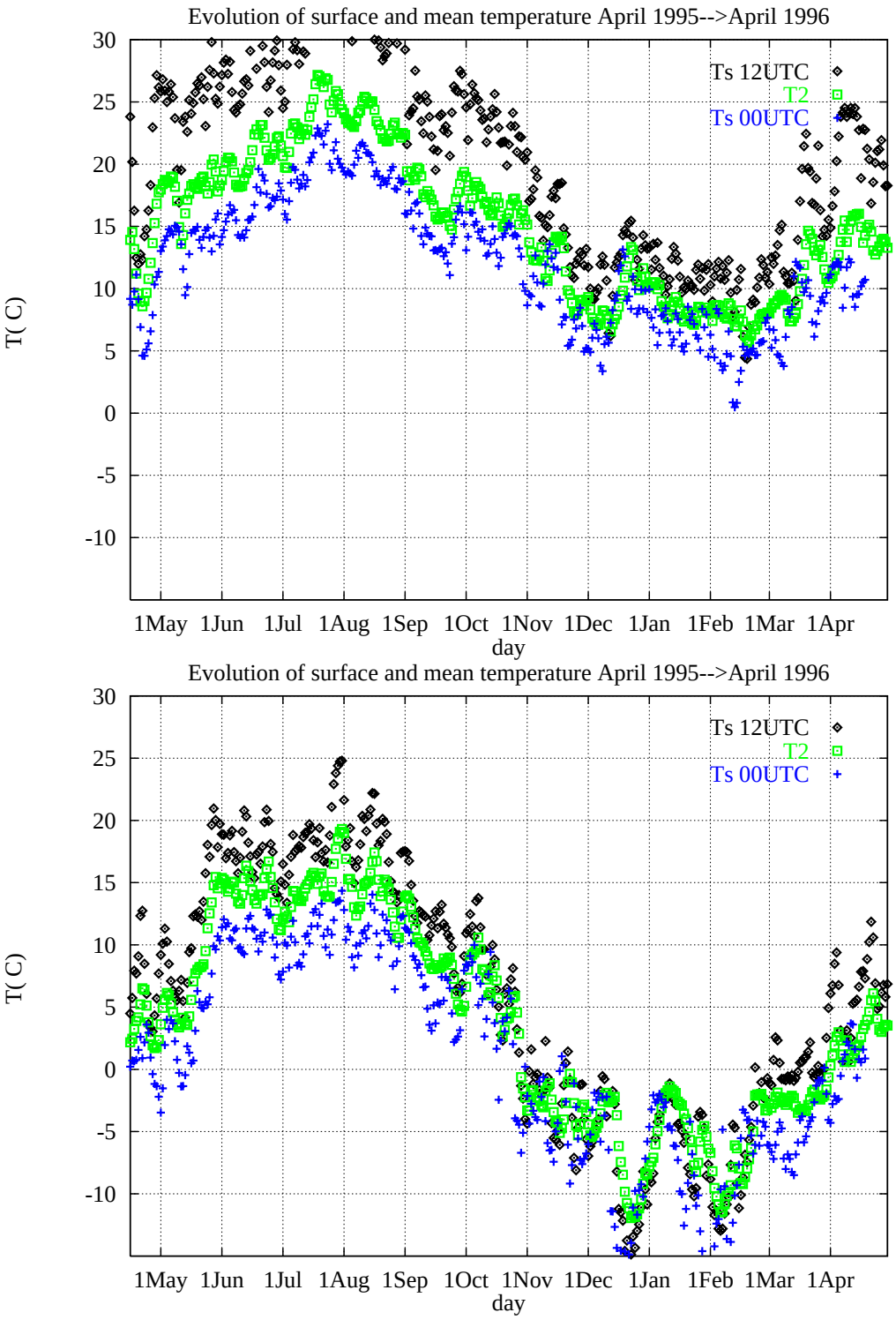

Figure 5: Daily evolution of 12 UTC (diamonds) and 00 UTC (crosses) surface and mean (squares) soil temperatures averaged for all grid points in the Iberian Peninsula (upper graph) and the Scandinavian area (lower graph). The assimilation experiment covers one full year (from 15 April 1995 to 30 April 1996).

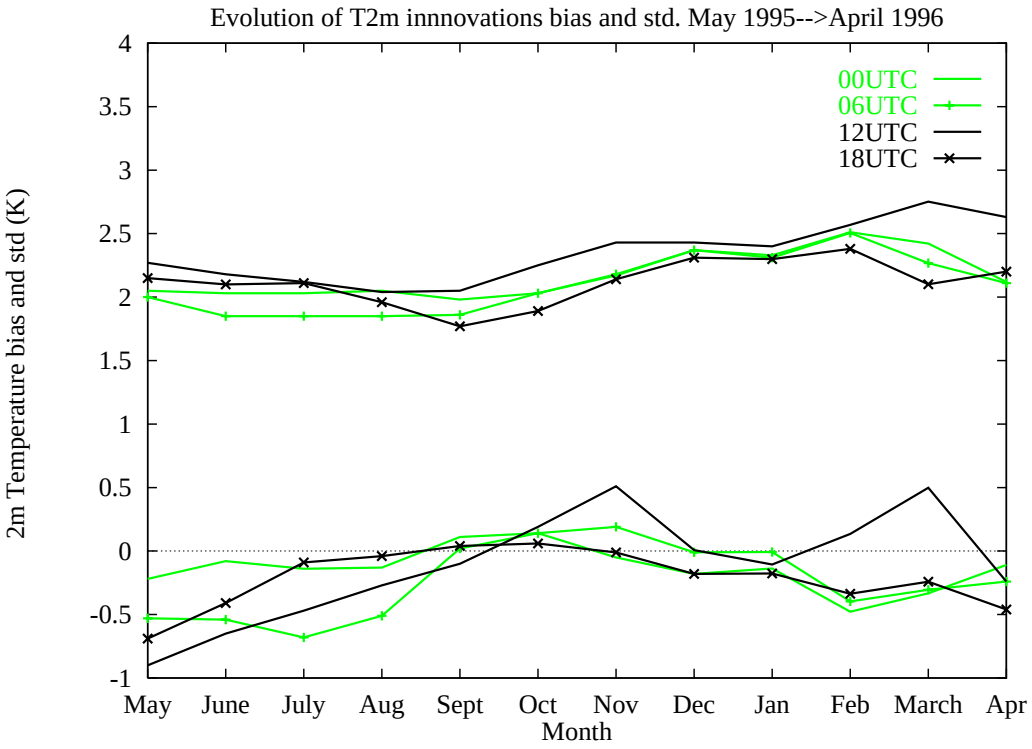

Figure 6: Monthly evolution of bias and standard deviation of observation minus first guess differences for 2-metre temperature at 00, 06, 12 and 18 UTC.

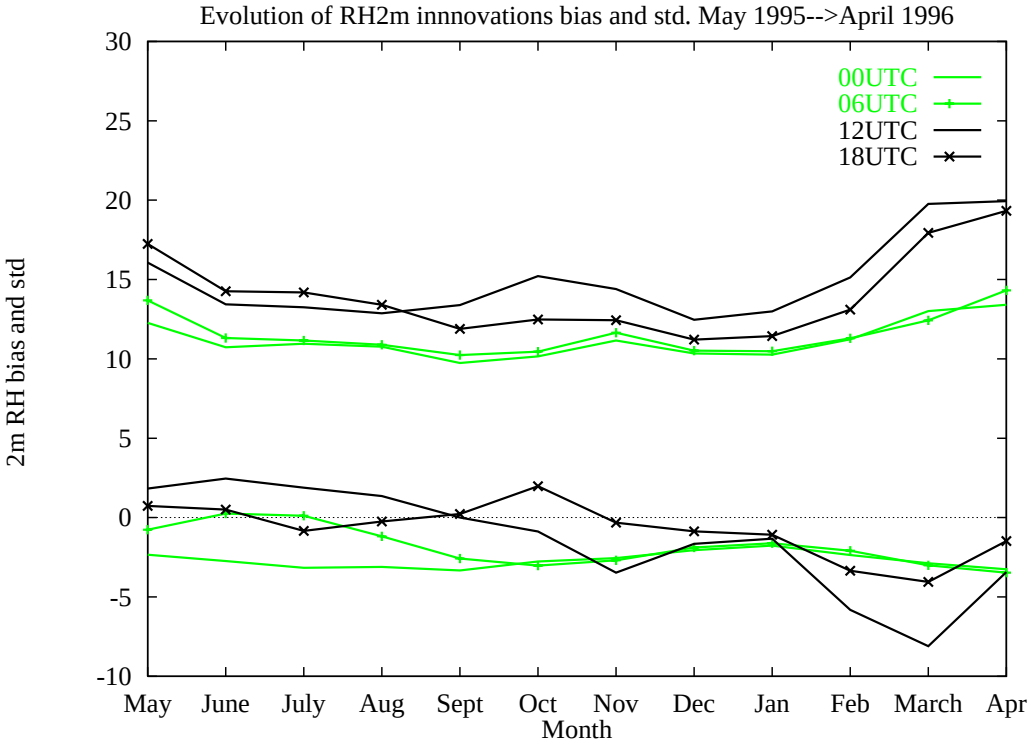

Figure 7: Monthly evolution of bias and standard deviation of observation minus first guess differences for 2-metre relative humidity at 00, 06, 12 and 18 UTC.

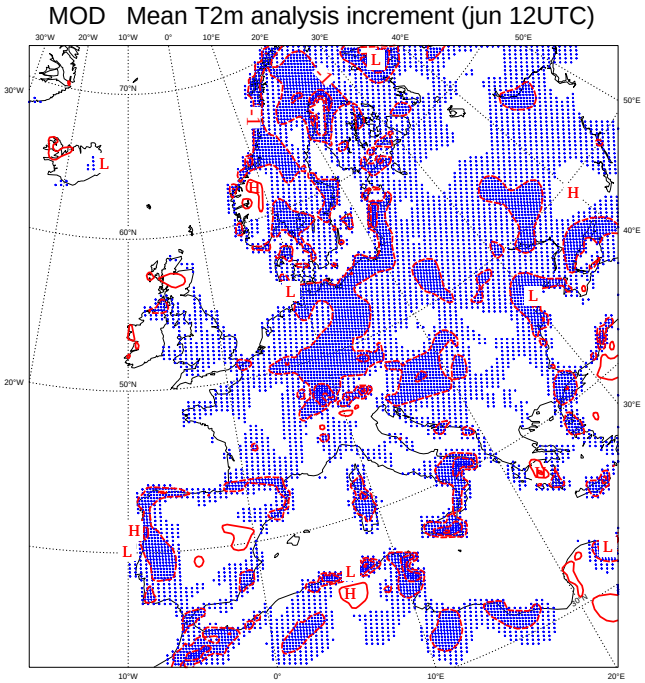

Figure 8: Mean analysis increments at 12 UTC of 2-metre for June 1995. Dashed lines correspond to negative analysis increments (too warm first guess) [starting from -1K]. Positive analysis increments (too cold first guess) are represented by solid lines [starting from +1K]. Shaded areas correspond to negative analysis increments. Contour interval is 1K.

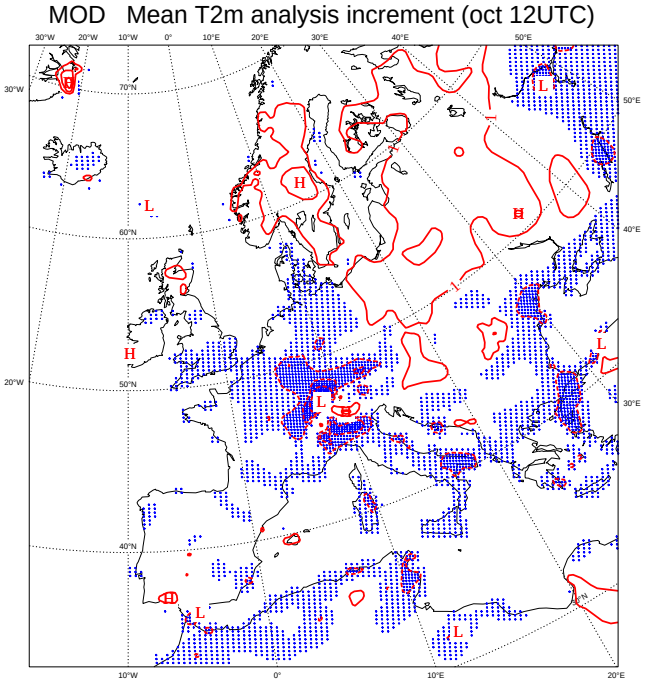

Figure 9: The same as Fig. 8, but for October 1995.

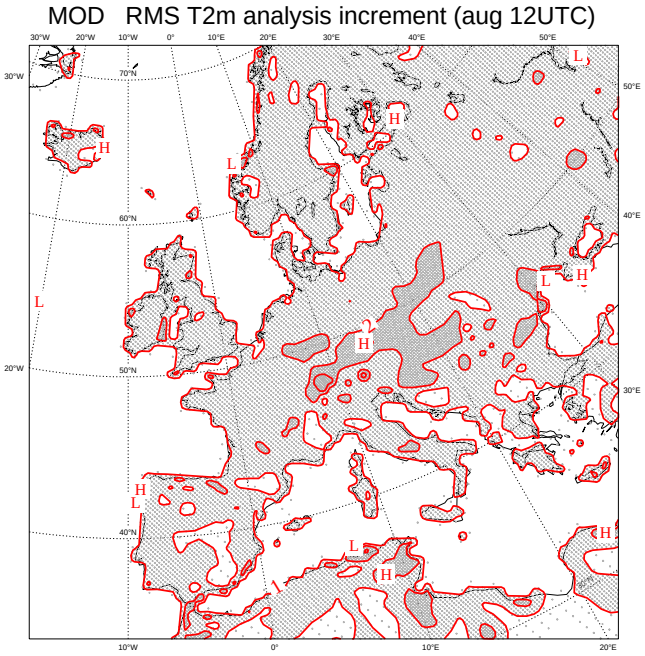

Figure 10: Root mean square of 2-metre temperature analysis increments at 12 UTC of 2-metre for August 1995. Contour interval is $1K$.

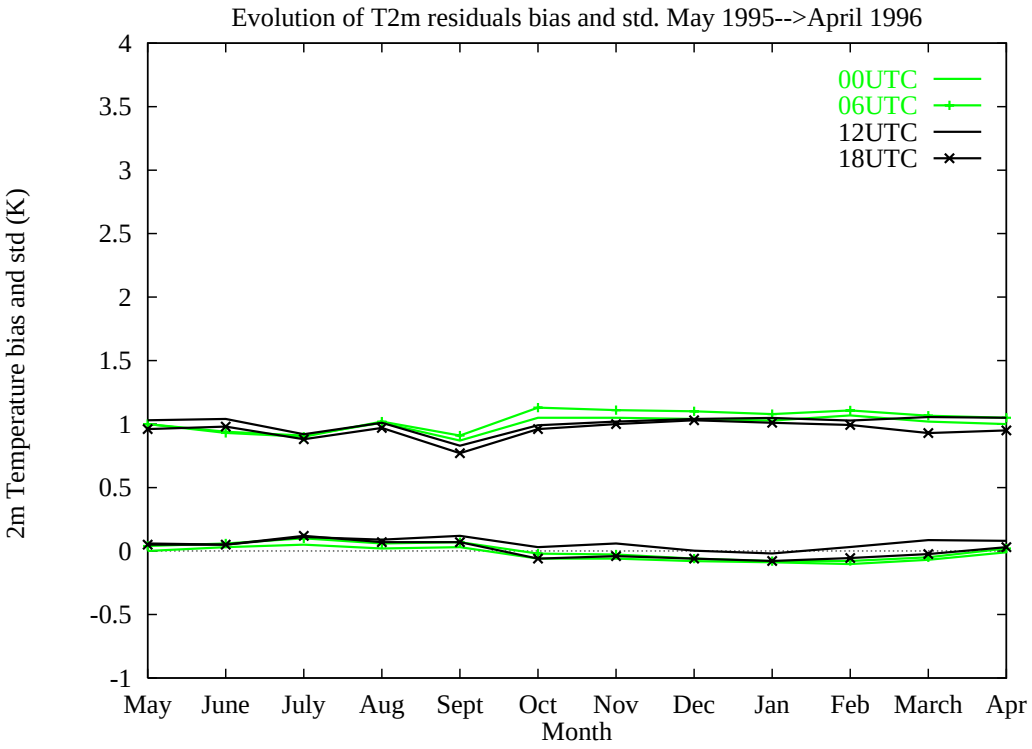

Figure 11: Monthly evolution of bias and standard deviation of observation minus analysis differences for 2-metre temperature at 00, 06, 12 and 18 UTC.

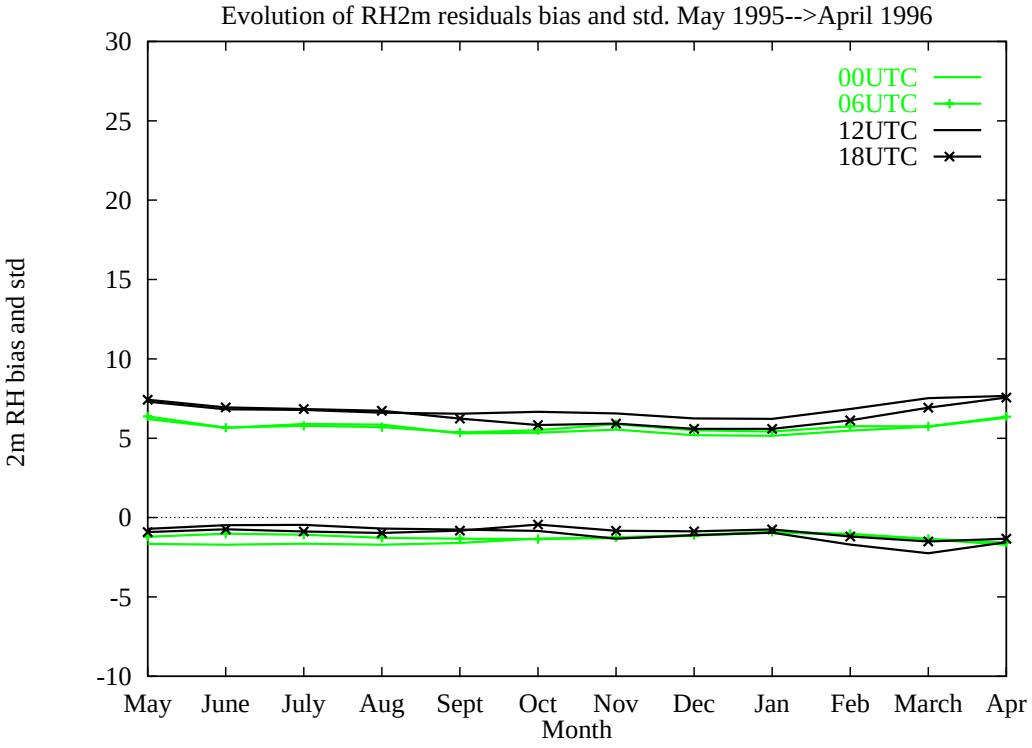

Figure 12: Monthly evolution of bias and standard deviation of observation minus analysis differences for 2-metre relative humidity at 00, 06, 12 and 18 UTC.

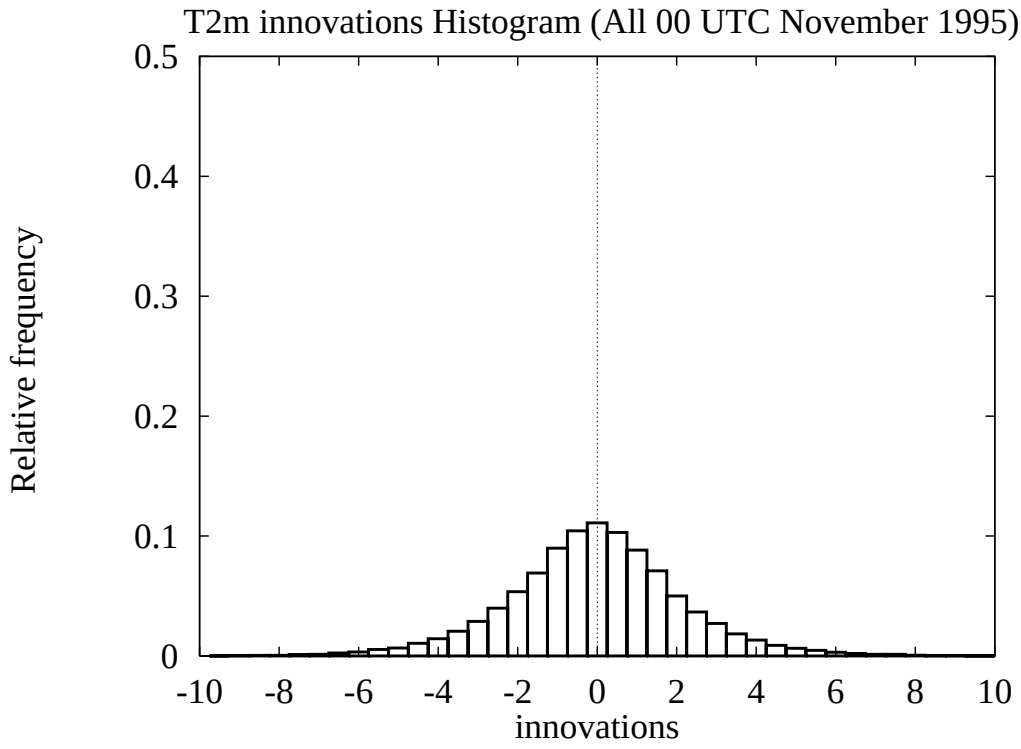

Figure 13: Histogram of 2-metre temperature innovations (unit: K) at 00 UTC in November 1995. Only observation minus first guess differences from accepted observations are considered here.

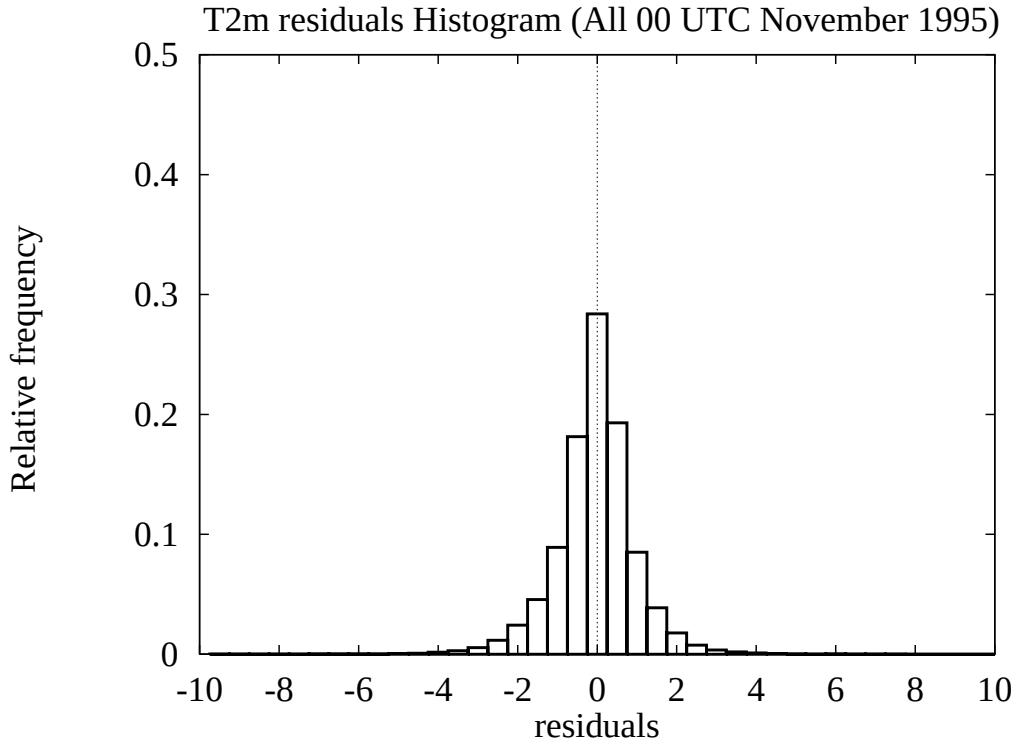

Figure 14: Histogram of 2-metre temperature residuals (unit: K) at 00 UTC in November 1995. Only observation minus analysis differences from accepted observations are considered here.

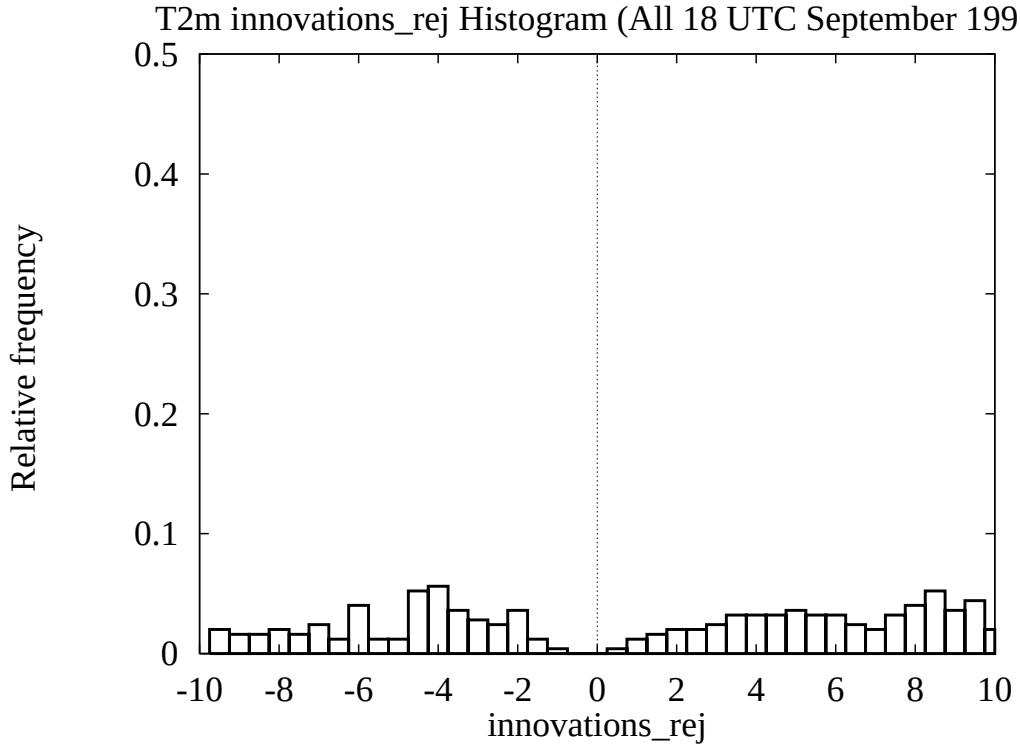

Figure 15: Histogram of 2-metre temperature innovations (unit: K) at 18 UTC for rejected observations in September 1995. Only observation minus first guess differences from rejected observations are considered here.

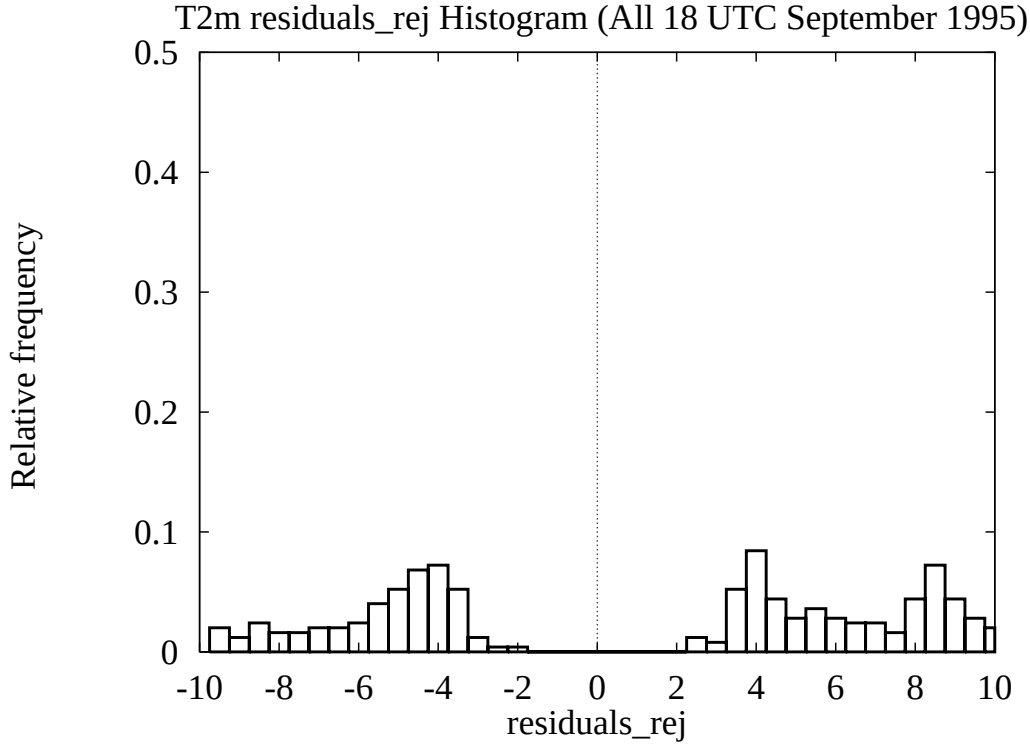

Figure 16: Histogram of 2-meter temperature residuals (unit: K) at 18 UTC for rejected observations in September 1995. Only observation minus analysis differences from rejected observations are considered here.

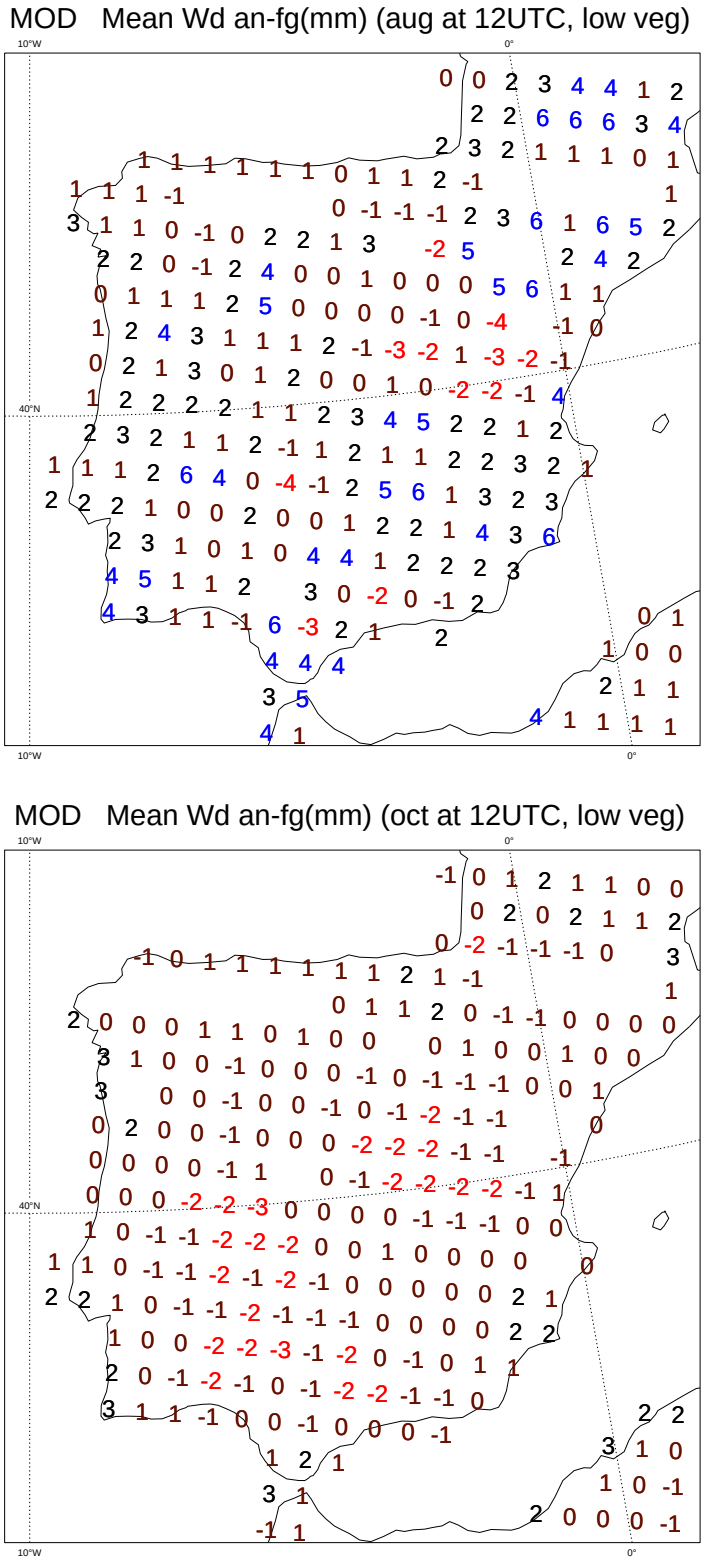

Figure 17: Mean soil water corrections at 12 UTC for the low vegetation tile over the Iberian Peninsula in August (upper map) and October (lower map) 1995. (blank areas correspond to grid points without any soil moisture correction over the period (see text for further explanations)). Units are *mm*.

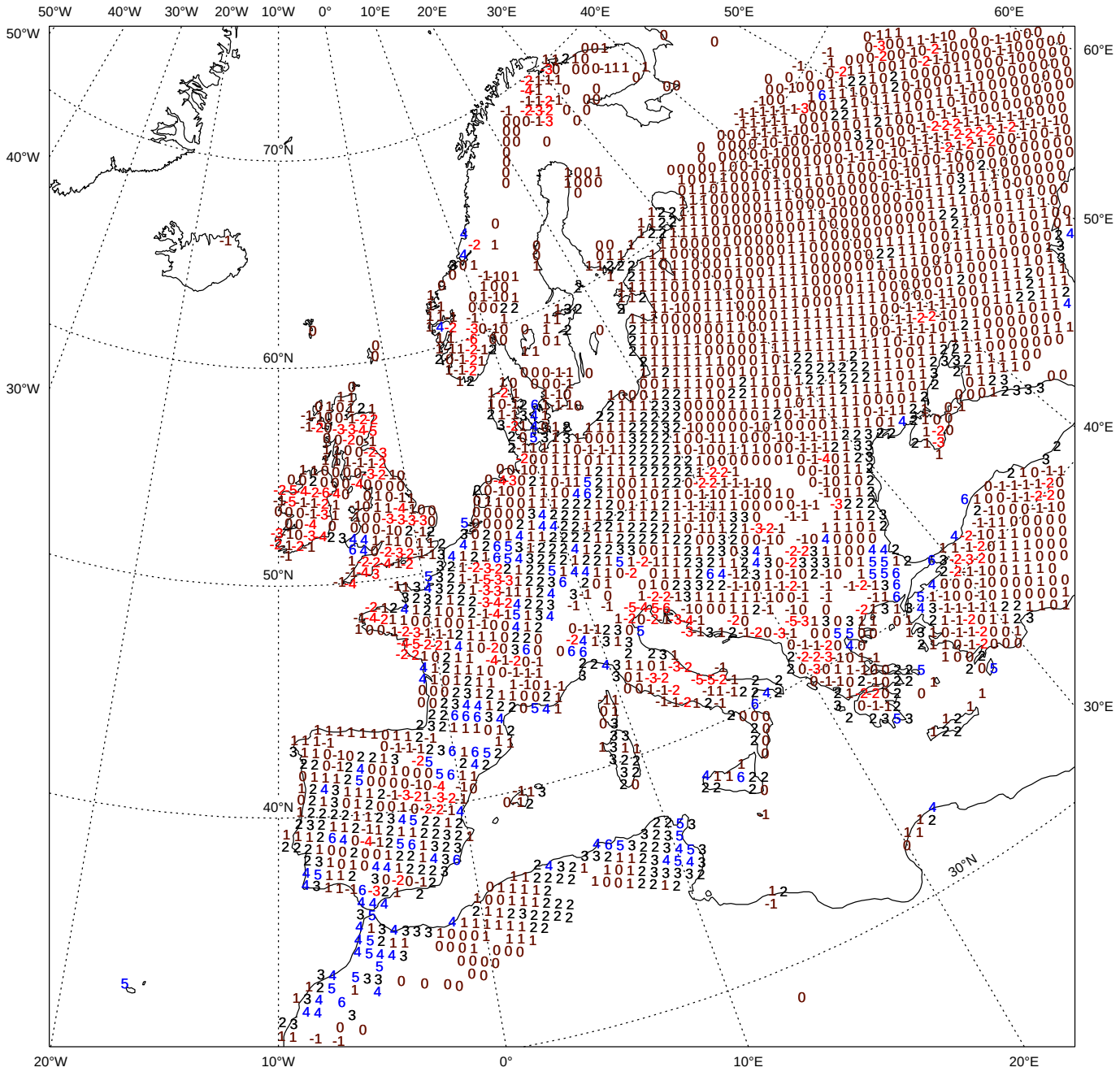

Figure 18: Mean soil water corrections at 12 UTC for the low vegetation tile in August 1995 (blank areas correspond to grid points either without low vegetation tile or without any soil moisture correction over the period (see text for further explanations)). Units are *mm*.

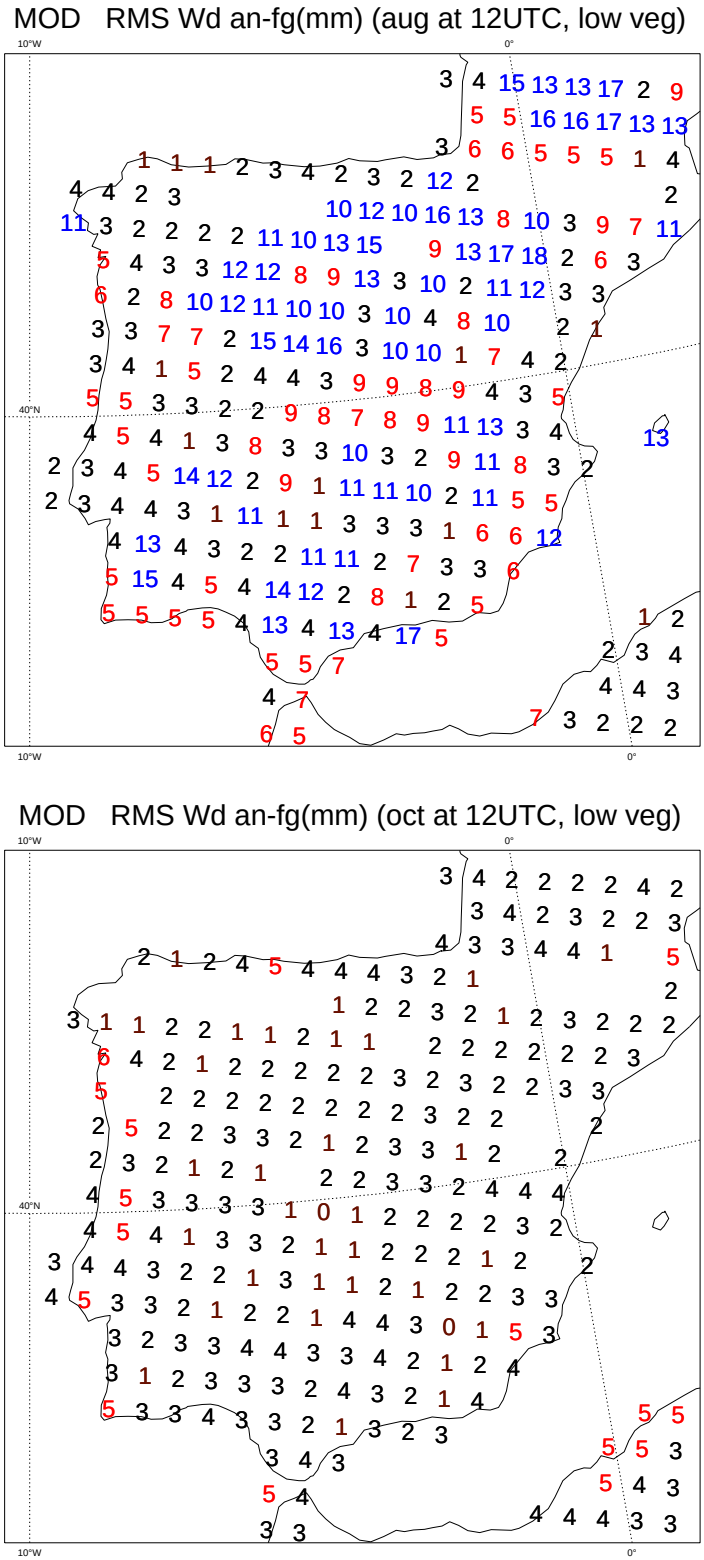

Figure 19: RMS soil water content analysis increments at 12 UTC for the low vegetation tile over the Iberian Peninsula in August (upper map) and October (lower map) 1995 (blank areas correspond to grid points without any soil moisture correction over the period (see text for further explanations)). Units are *mm*.

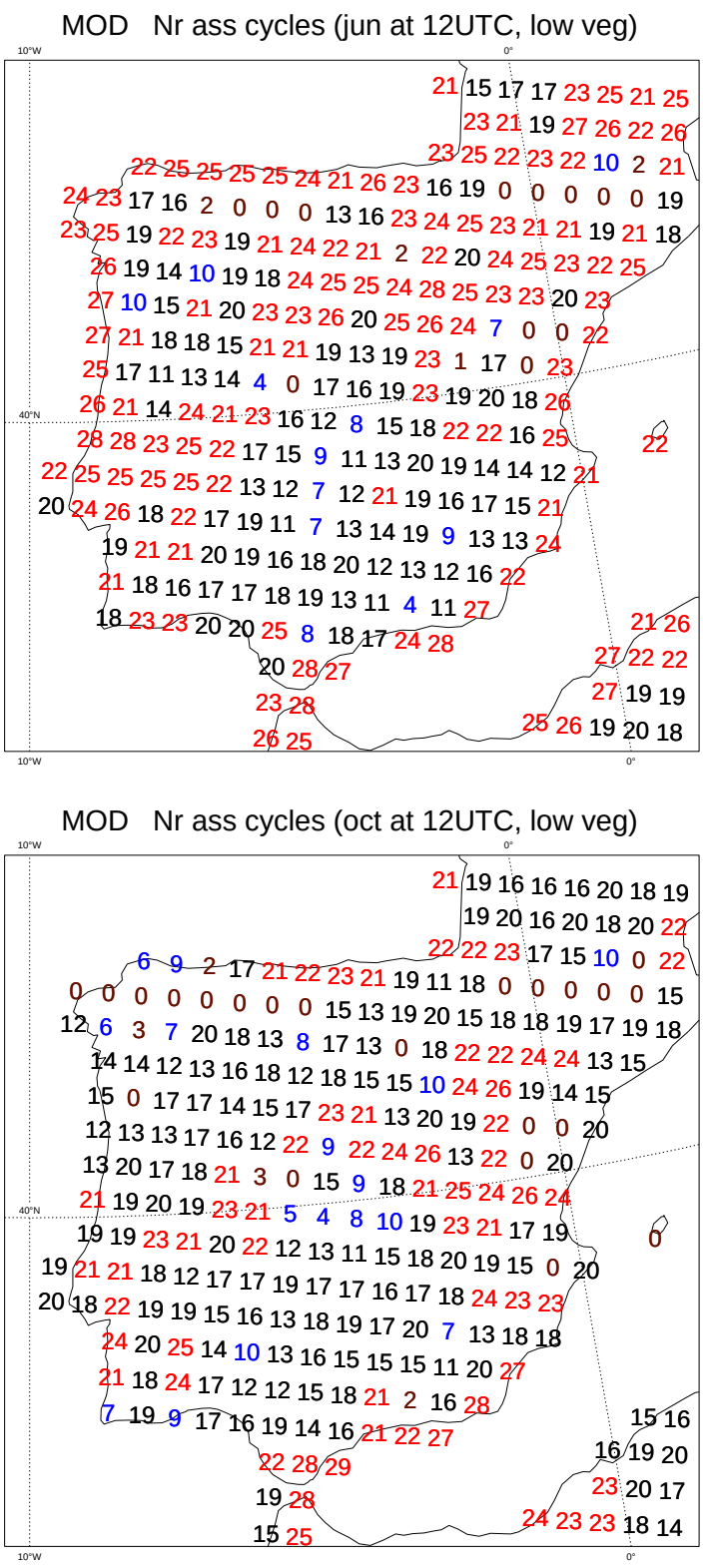

Figure 20: Number of effective soil water content corrections for the low vegetation tile at 12 UTC over the Iberian Peninsula in June (upper map) and October (lower map) 1995. Low vegetation tile.

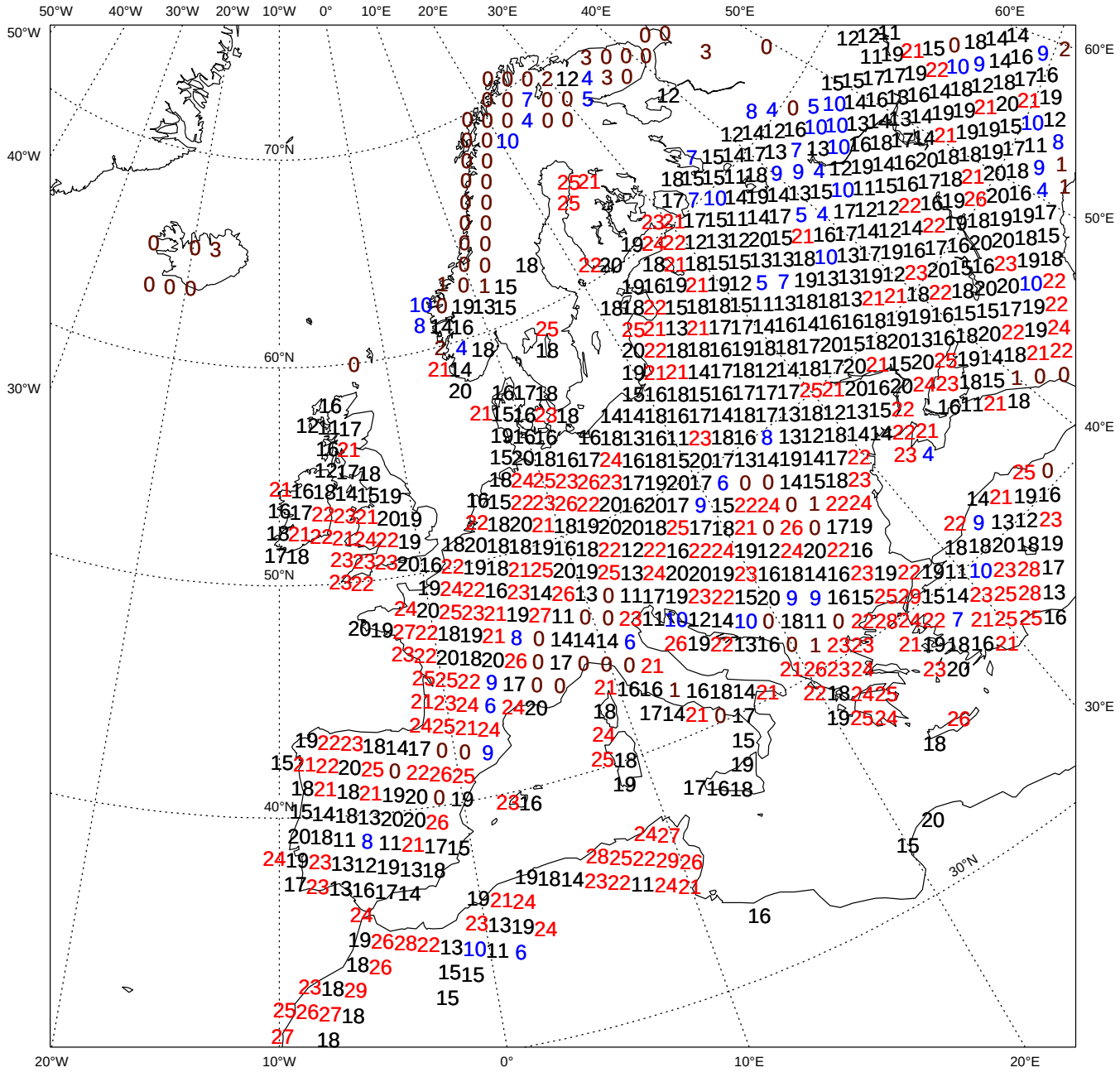

Figure 21: Number of effective soil water content corrections for the low vegetation tile (blank areas mean absence of the corresponding tile). Every second grid value is given in each direction.

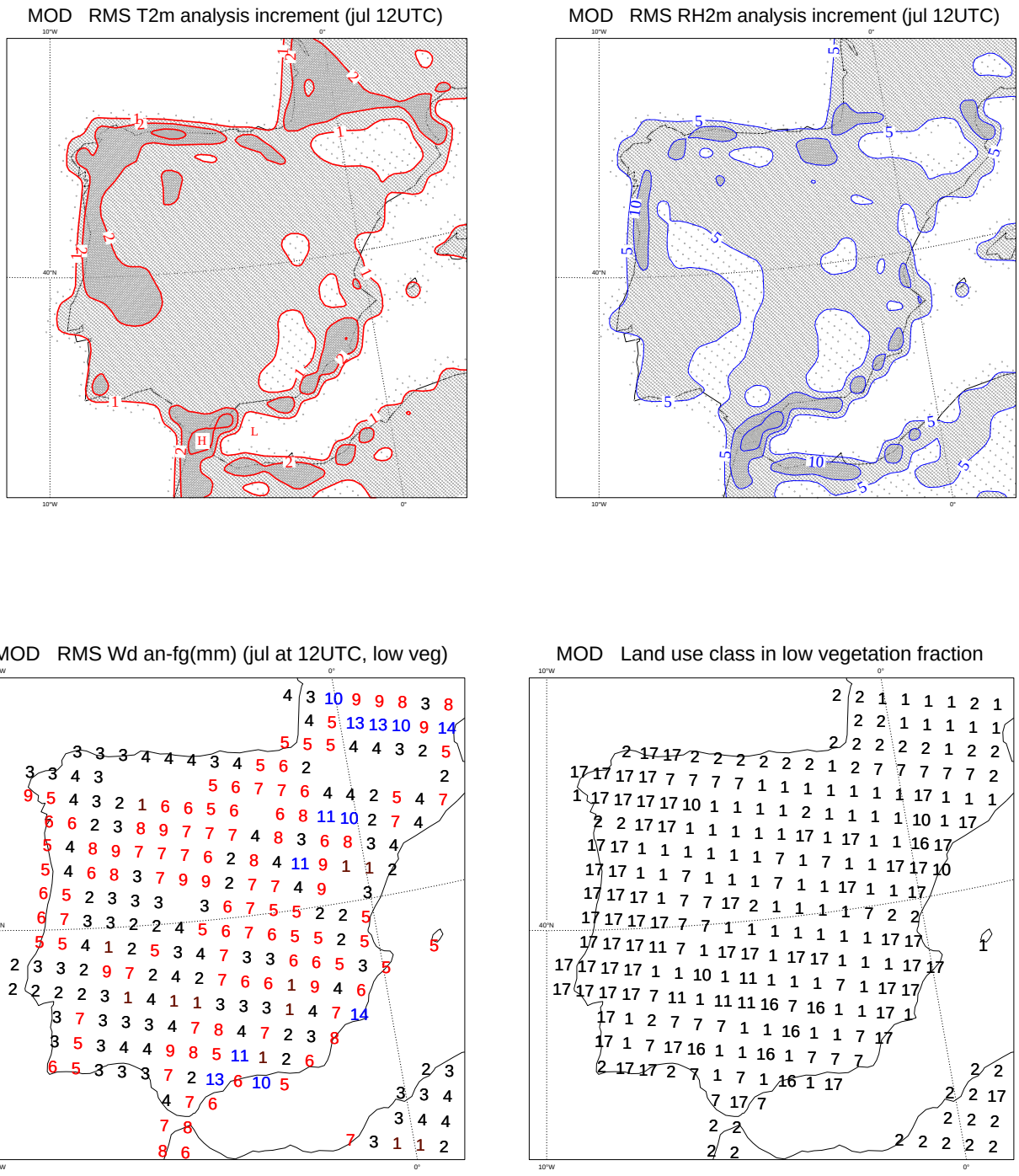

Figure 22: Upper maps: rms 2-metre temperature (left) and relative humidity (right) analysis increments in July 1995. Lower left map: rms of soil water content analysis increment in July 1995. Lower right map: land use class in low vegetation tile (indeces correspondence to vegetation types is indicated in Table 1).

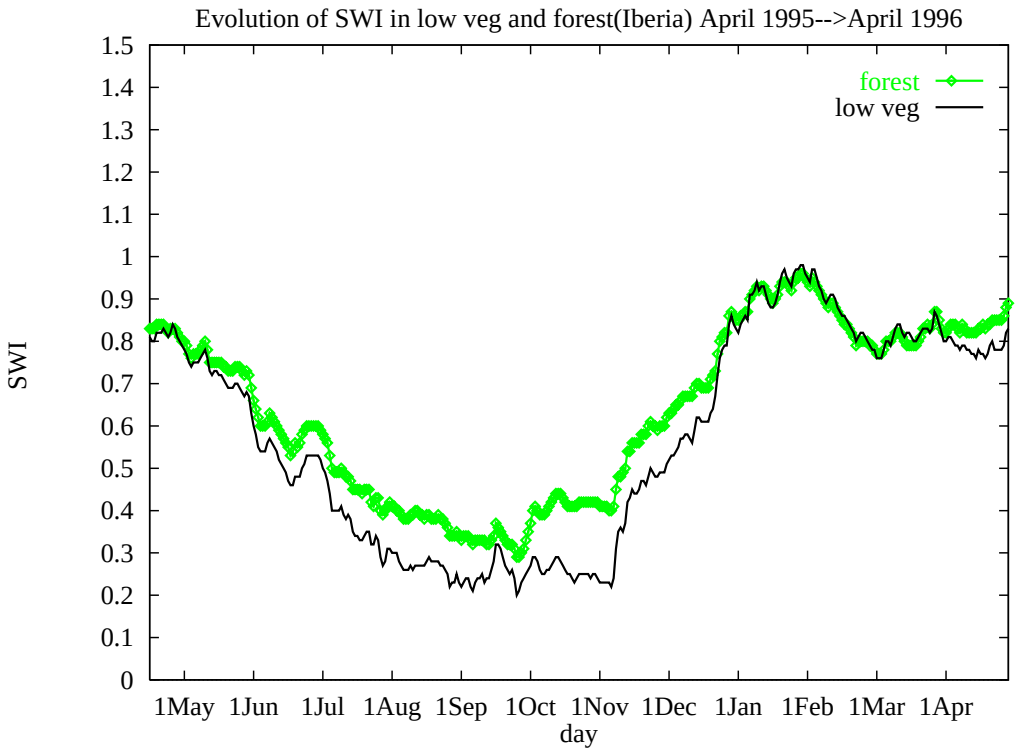

Figure 23: Daily evolution of total layer soil wetness index averaged for all grid points over the Iberian Peninsula. Values of low vegetation and forest fractions are represented separately.

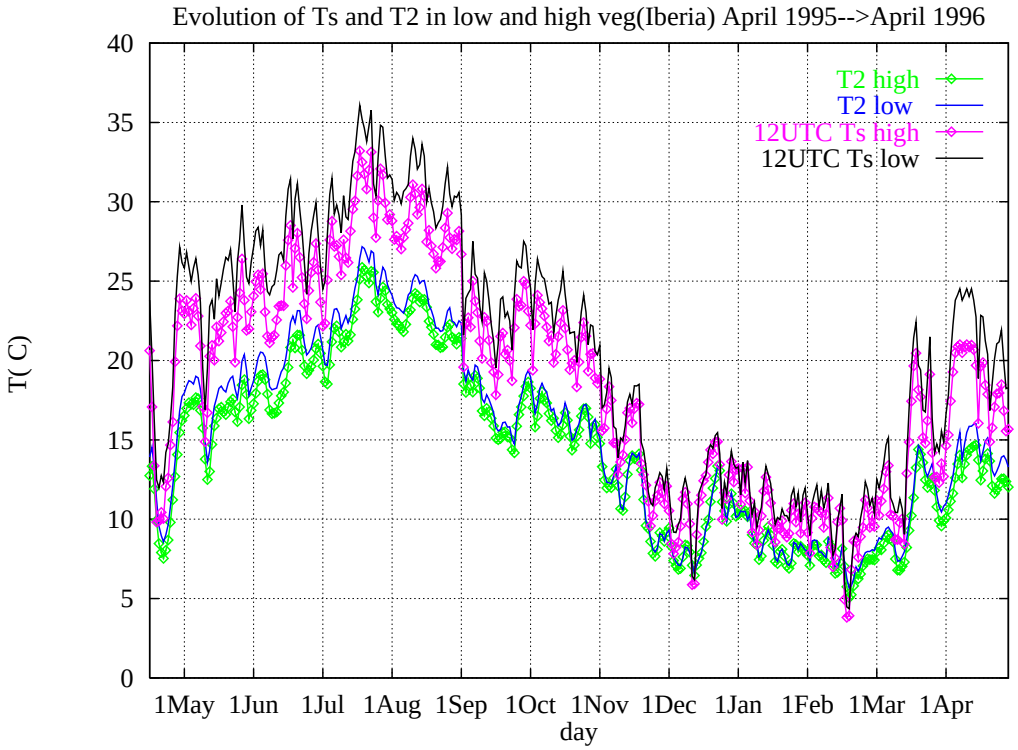

Figure 24: Daily evolution of 12 UTC surface and mean soil temperatures averaged for all land grid points over the Iberian Peninsula. Values of low vegetation and forest fractions are represented separately. All temperatures correspond to 12 UTC analysis.

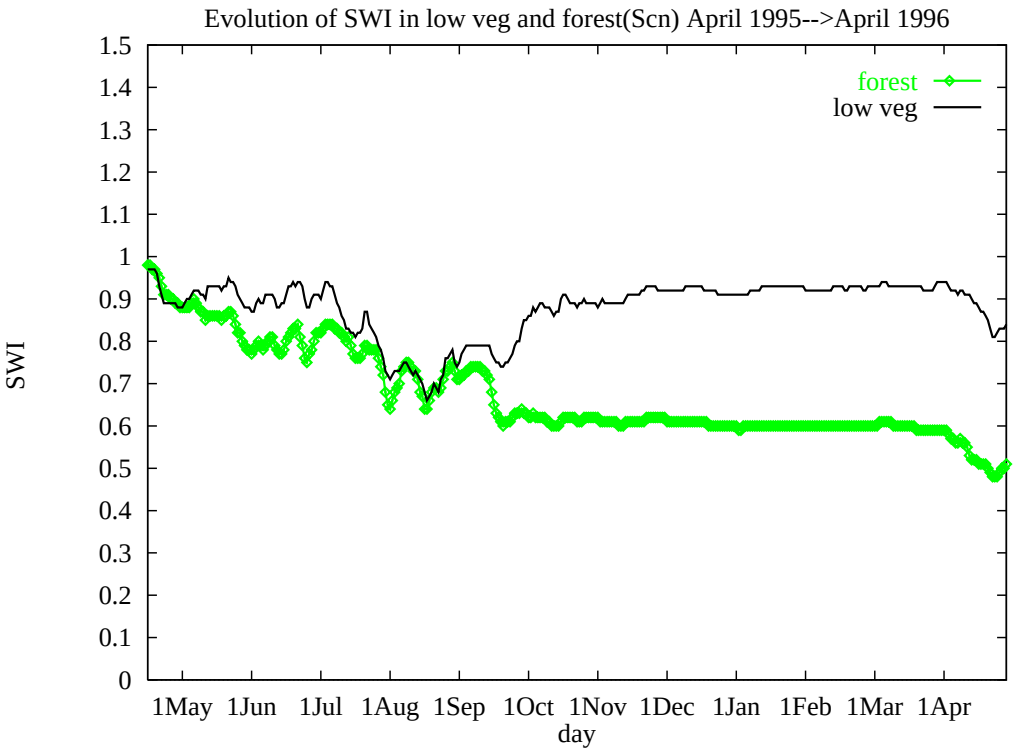

Figure 25: Daily evolution of total layer soil wetness index averaged for all grid points over Scandinavia. Values of low vegetation and forest fractions are represented separately.

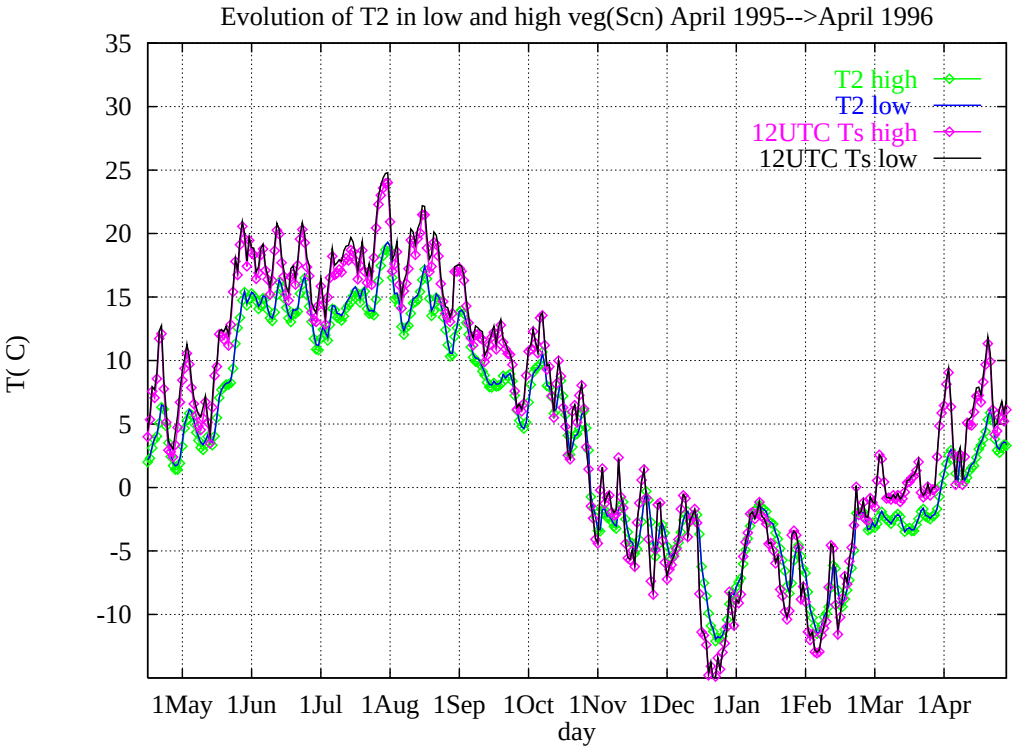

Figure 26: Daily evolution of 12 UTC surface and mean soil temperatures averaged for all land grid points over Scandinavia. Values of low vegetation and forest fractions are represented separately. All temperatures correspond to 12 UTC analysis.

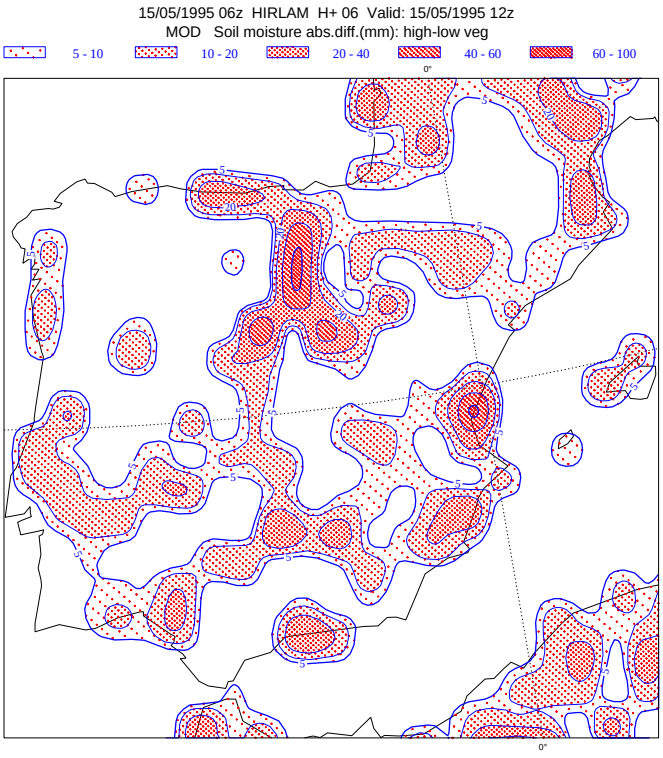

Figure 27: Absolute difference of total soil moisture (units: mm) between low vegetation and forest tiles in the same grid box corresponding to 15 May 1995 at 12 UTC. (Soil depths of both tiles are normalized to $1m$).

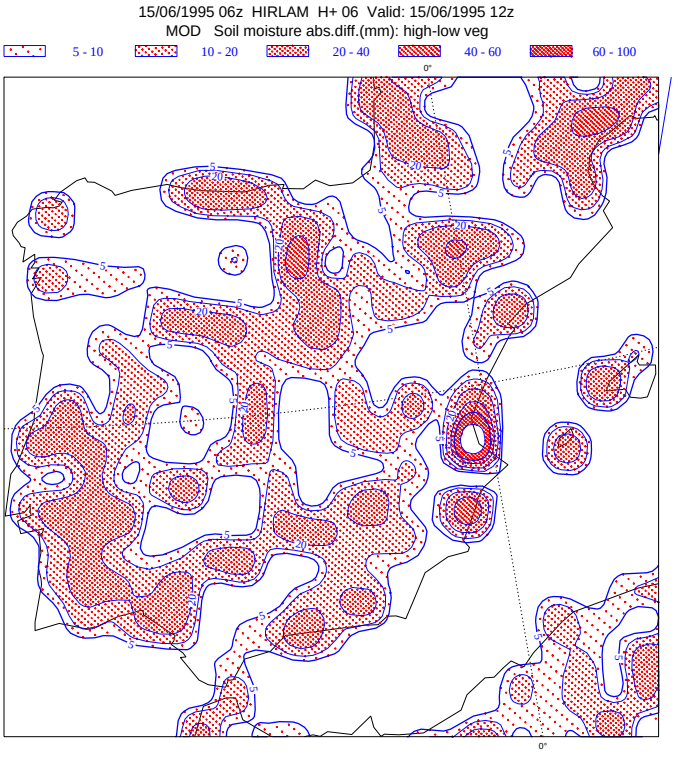

Figure 28: As in Fig. 27, but for 15 June 1995 at 12 UTC.

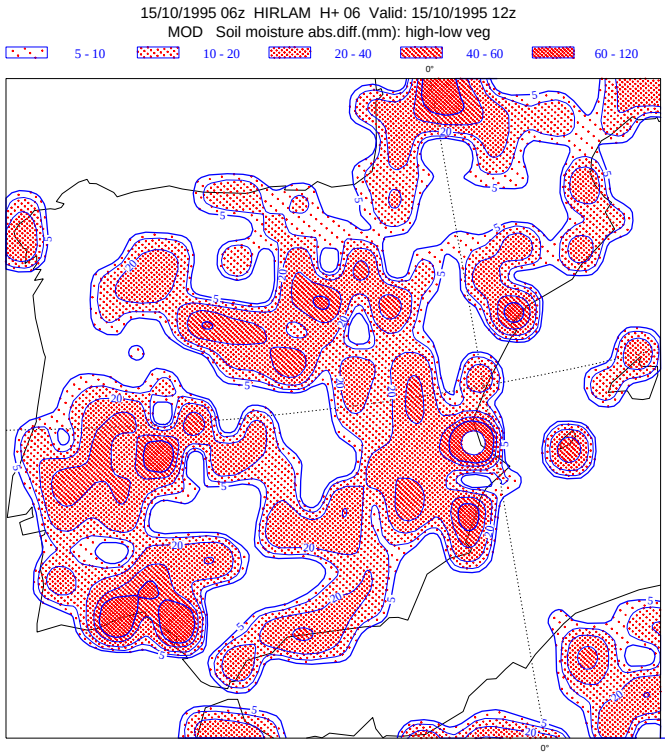

Figure 29: As in Fig. 27, but for 15 October 1995 at 12 UTC.

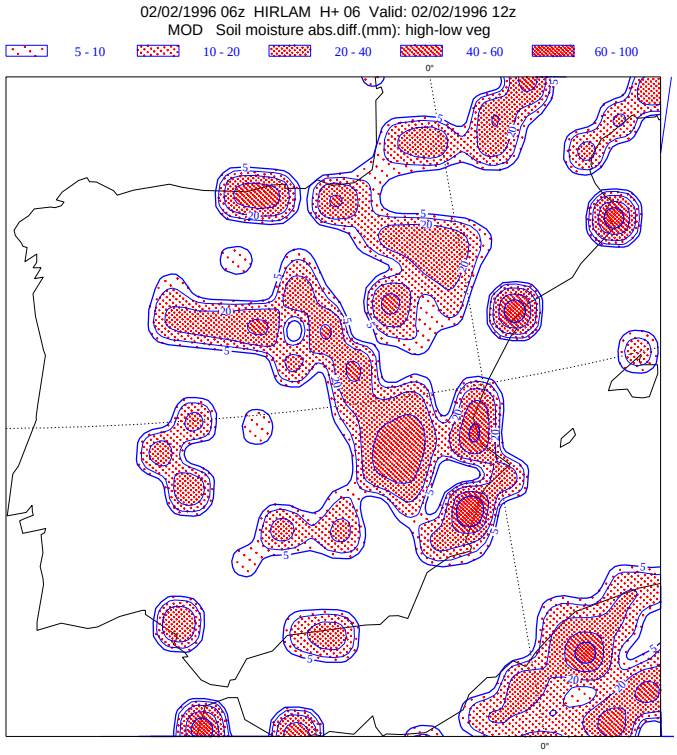

Figure 30: As in Fig. 27, but for 2 February 1996 at 12 UTC.

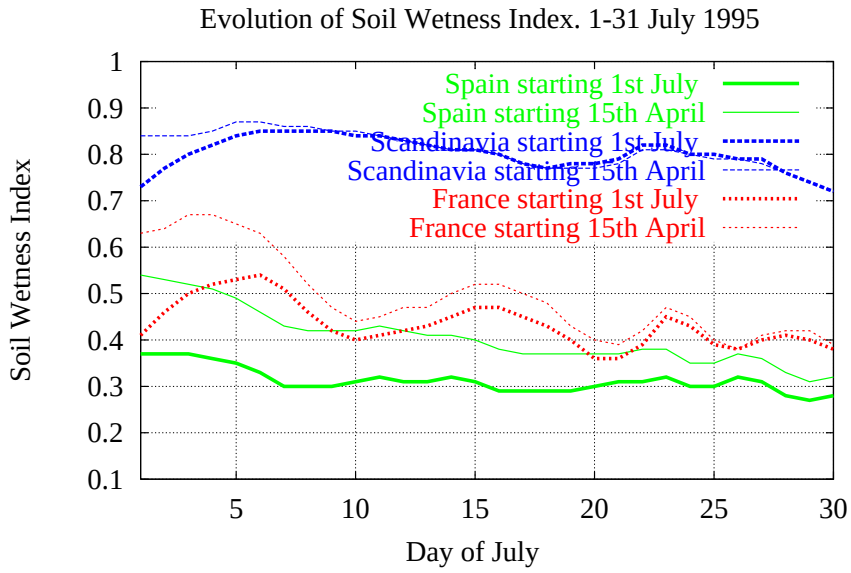

Figure 31: Daily evolution of soil wetness index (SWI) averaged for all grid points in some European areas (Spain, France and Scandinavia) as seen by 12 UTC analysis in experiments started on 15th of April and on 1st of July 1995.

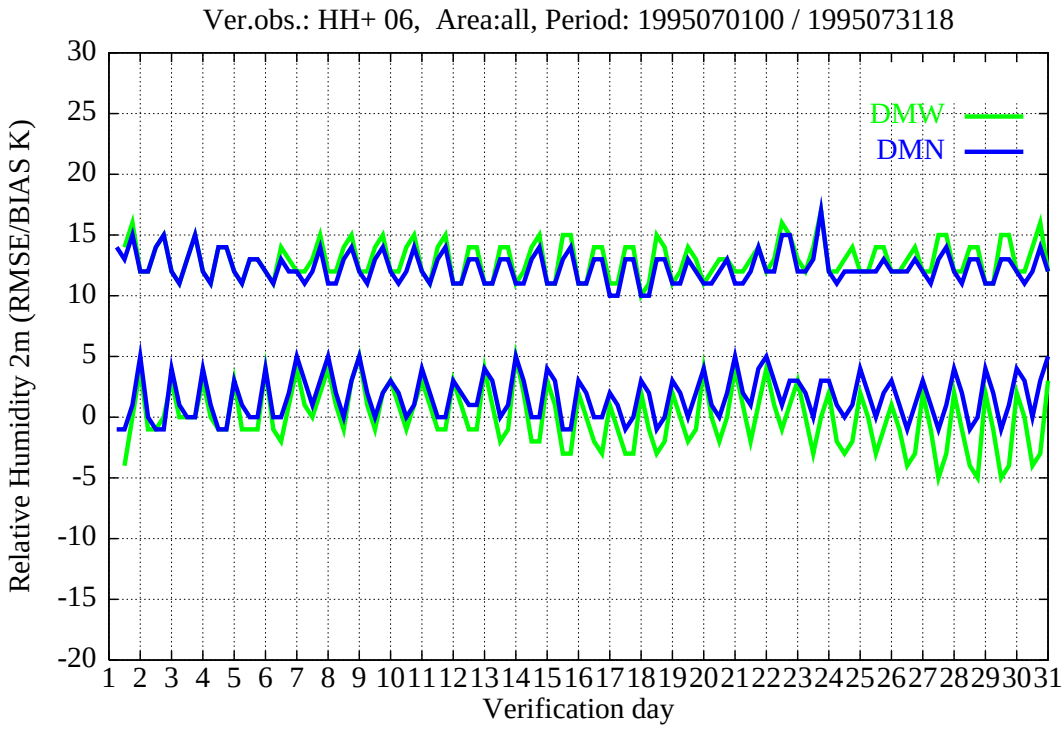

Figure 32: Daily evolution of H+6 2-metre relative humidity forecast errors. Bias and rms scores were calculated using all observations in the model area. DMW experiment was run without soil moisture correction in the analysis step. DMN experiment was performed with soil moisture assimilation. Both DMN and DMW experiments were started on 1st of July 1995.